Electron-Positron Pair Production in Relativistic Heavy Ion Collisions

Gerhard Baur, [a] Kai Hencken, [b,c] and Dirk Trautmann [b]

[a] *Forschungszentrum Jülich, Jülich, Germany*
[b] *Universität Basel, Basel, Switzerland*
[c] *ABB Corporate Research, Baden Dättwil, Switzerland*

Abstract

In recent years, a large number of papers have appeared that dealt with e^+e^- pair production in heavy ion collisions at high energies. To a large extent these studies were motivated by the existence of relativistic heavy ion accelerators all over the world. There pair production can be studied in so called "ultra-peripheral collisions", where the ions do not come close enough to interact strongly with each other. Various different methods have been used and it is the purpose of this review to present a unified picture of the present status of the field. The lowest order Born result has been known for more than seven decades. The interest and focus is now on higher order effects for values of $Z\alpha \lesssim 1$, where Z is the charge number of the ion. A similar problem appears for the Bethe-Heitler process, the production of e^+e^- pairs in photon-nucleus collisions. It was solved essentially some five decades ago by Bethe and Maximon. The result of Bethe and Maximon can also be recovered by summing over a class of Feynman diagrams to infinite order. These results can be used for a study of Coulomb corrections in nucleus-nucleus collisions. Indeed, the major part of these corrections have a structure closely related to the Bethe-Maximon solution. There are additional terms which give a small contribution to the total cross section at high energies. Their importance can be enhanced by concentrating on small impact parameters. An interesting exact solution of the one-particle Dirac equation in the high-energy limit was found independently by several authors. This led to some discussion about the interpretation of these results within QED and the correct regularization necessary to get the correct result. The dust of previous debates has settled and, indeed, a consistent picture has emerged. Another interesting higher order effect is multiple pair production, which we also discuss. We compare experimental results obtained recently at RHIC for free and bound-free pair production with theoretical results. We also make some more remarks on the physics of strong electric fields of longer duration. A new field is opened up by ultra-intense laser pulses. We argue that due to the short interaction time in ultraperipheral heavy ion pair production can be well understood in the frame of QED perturbation theory.

Key words: Electron-Positron Pair Production, QED of strong fields, Coulomb Corrections, Multiple Pair Production, Relativistic Heavy Ion Collisions, Ultraperipheral Collisions.

Contents

1 Introduction, overview and purpose

Quantum electrodynamics (QED) is the best-tested theory we have [1,2,3,4]. It is a quantum field theory which describes the gauge invariant interaction of charged particles with photons. With this theory one is able to describe high precision experiments like the Lamb shift and the magnetic moments of the electron and muon with great accuracy. In the present review we are dealing with the fundamental process of particle production in high energy scattering processes. Experiments up to now have been not very accurate in their results. Also, the theoretical precision was not very high. This is not due to principal problems of the underlying theory, the QED. It is more related to technical difficulties, as we shall see in the following. An especially interesting process is the production of electron-positron pairs under various conditions.

Positrons were first observed in cosmic ray interactions in 1932 [5]. The theoretical calculation of e^+e^- pair production in fast nucleus-nucleus collisions goes back to the early days of QED [6]. The full result in lowest order perturbation theory (Born approximation) is due to Racah [7]. These results are also discussed in [8]. In those calculations the pair production is due to the collision of a pair of (virtual) photons. The theoretical, as well as, experimental interest in these processes was spurred in the last decades by the relativistic heavy ion facilities AGS at Brookhaven, SPS at CERN and more recently RHIC at Brookhaven and LHC at CERN. It was realized that the old lowest order answers are no longer sufficient for the strong Coulomb field surrounding the heavy ions at these high energies. There are (new) sizeable and interesting higher order effects.

The subject of this review is precisely the situation envisaged in these early works of the thirties of the past century, i.e. pair production in high energy nucleus-nucleus collisions. The theoretical treatment now concentrates on higher order effects. One type of effects is the influence of higher orders on the one-pair production. Very similar "Coulomb corrections" have been discussed already before in pair production by a single (real) photon in the Coulomb field of a nucleus. As we will see a lot of the experience gained there can also be applied to the case of two heavy ions. Another — new and more spectacular — effect is the production of many pairs in a single collisions, clearly a higher order effect. Various groups have been working on these problems in the past two decades using various methods and approximations. The main purpose of this review is to discuss these various methods and to establish the relationship of the different approaches. Since QED is a well established theory, such a connection is to be expected.

Before dealing specifically with our subject of relativistic heavy ion collisions, it is appropriate to put the present subject of e^+e^- production in relativistic

nucleus nucleus collisions into a wider perspective: slow collisions of heavy ions of charge numbers Z_1 and Z_2 are a way to create, at least for a short time, atoms with a charge $Z_{\text{united atom}} = Z_1 + Z_2$. It is of special interest to study collisions where the sum of the charges $Z_{\text{united atom}} > 137$ (173). In these collisions so called "overcritical fields" are reached for some time where spontaneous e^+e^- production is possible, see [9] or the detailed review of this field in [10]. The supercritical field is reached for a charge $Z = 137$ in the case of a point nucleus, where one may say that the $1s_{1/2}$-level dives into the negative energy continuum. For extended nuclei with a finite radius, this limit is reached at about $Z = 173$ [9].

The paradigm of e^+e^- pair production is the Schwinger mechanism: the production of pairs in a constant spatially uniform electric field [11], see Fig. 1. To reach a sizeable rate for spontaneous production of e^+e^- pairs a field strength of the order of or above a certain critical field strength E_c is required. The rate of (one) pair production per unit volume and time for a given constant field E is given by [12]

$$\frac{d^4 n_{e^+e^-}}{d^3 x dt} \sim \frac{c}{4\pi^3 \lambdabar^4} \exp(-\pi \frac{E_c}{E}), \tag{1}$$

where the critical field strength is given by

$$E_c = \frac{m^2 c^3}{e\hbar} \simeq 1.3 \times 10^{16} V/cm. \tag{2}$$

The electron mass is denoted by m and its Compton wavelength is given by $\lambdabar = \frac{\hbar}{mc}$. This formula clearly shows the non-perturbative nature of the problem: there is no power series expansion of the e^+e^- production rate in terms of the electric field strength E. With new developments in laser physics it seems that this field strength can be reached, e.g., at the FEL at DESY and the interest has grown enormously, both in theory and experiment [13,14]. In contrast to relativistic heavy ion collisions, the created fields in this case are of a comparatively long duration. This is made more quantitative in [15] and will be dealt with in Sec. 7.

The main purpose of relativistic heavy ion collisions is the production and observation of the quark gluon plasma which yields information about QCD at high temperature and densities. It has gradually been realized over the last decades that the very strong electromagnetic fields present in distant heavy ion collisions are also useful: they provide a strong flux of equivalent photons for photon-hadron and photon-photon physics with hitherto unknown energies. The term "ultraperipheral collisions" (UPC) has been coined to describe collisions where the impact parameter is larger than the sum of the two nuclei: in this case only electromagnetic interactions occur between the ions.
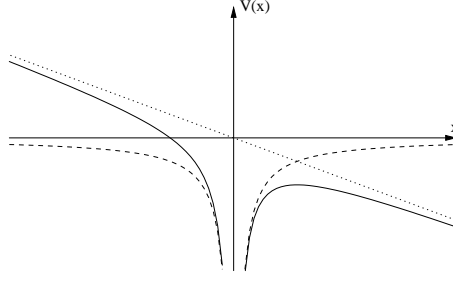
5

Fig. 1. Pair production in a strong static field E. The total potential is given by the potential energy (solid line) of the electron in the binding potential $V(x)$ (dashed line) and in the static electric potential eE. We may consider the electron bound by a potential of depth $\sim 2mc^2$. In the Schwinger process the electron tunnels through the barrier and an e^+e^- pair is created, see [12].
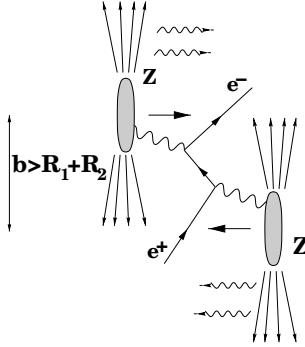

Fig. 2. The electromagnetic fields of two heavy ions in an ultraperipheral collision. These fields can be decomposed into a spectrum of quasireal photons (Weizsäcker-Williams approximation). The collision of two photons gives rise to a dilepton pair. The collision of photons radiated from each nucleus are a copious source of e^+e^- pairs.

One special case of photon-photon physics in UPCs is e^+e^- production, see Fig. 2. Due to the smallness of the electron mass e^+e^- pair production is very copious, it is of the order of kilobarns under RHIC and LHC conditions. The physics of "ultraperiphal collisions" is reviewed in [16,17,18,19] and [20]. A recent workshop at ECT*/Trento,Italy was devoted to the subject of UPC [21]. The status of e^+e^- pair production was also discussed there, see [22].

Let us make some order of magnitude estimates of the fields acting in the case of relativistic heavy ion collisions: the electromagnetic fields encountered in these collisions are extremely strong, they are of the order of

$$E_{\max} \simeq \frac{Ze\gamma}{b^2}, \tag{3}$$

where we assume that the ions move on straight line trajectories with impact parameter b and γ is the Lorentz factor in the collider system. With the values of $Z = 79$, $b = b_{min} = 15 fm$ and $\gamma = 100$, which are appropriate for RHIC, we

find a maximum field strength of $E_{\max} = 4.9 \times 10^{16} V/cm$. For LHC conditions ($Z = 82, b_{min} = 15fm, \gamma = 3000$) we get $E_{\max} = 1.5 \times 10^{18} V/cm$. These are the values viewed in the collider frame. Viewed from the other nucleus the corresponding Lorentz factor is $\gamma_{ion} = 2\gamma^2 - 1$ and the electric fields are even larger by a factor of γ.

These field strengths are comparable to the critical field E_c for the Schwinger mechanism. However, these fields act only for a very short time

$$\Delta t \simeq \frac{b}{\gamma v}, \tag{4}$$

where $v \sim c$ is the ion velocity. For $b = \lambdabar \simeq 386$fm one obtains the values of $\Delta t \simeq 10^{-23} s$ for RHIC and $\Delta t \simeq 3 \times 10^{-25} s$ for LHC conditions, respectively. The momentum transfer Δp given to a test particle with a charge e along a path with impact parameter b is independent of γ. For $v \sim c$ and $b = \lambdabar$ it is only modest

$$\Delta p \sim e E_{max} \Delta t \sim \frac{Ze^2}{bv} \sim Z\alpha mc. \tag{5}$$

This small value gives a strong hint that the use of perturbation theory is still appropriate in contrast to the situation of the Schwinger mechanism mentioned above. Surely there are higher order effects, but they can be dealt within higher order perturbation theory, see, e.g., [23]. One goal of this review is the explanation of the results for the effects beyond lowest order perturbation theory. An obvious question is about the transition from the slow to the fast collisions.

In section 2 we recall a simpler but intimately related problem: the Bethe-Heitler process, i.e. the photoproduction of e^+e^- pairs in the nuclear Coulomb field. It shows already many of the characteristic aspects of the heavy ion case. Higher order effects were treated in [24,25] by using the Sommerfeld-Maue wave functions: these wave functions are appropriate high energy solutions of the Dirac equation and thus take higher order effects into account to all orders. This is a textbook example (see e.g. [26]). It was shown in [27] how this approach is related to the usual Feynman graph technique.

In section 3 we come back to the case of ultraperipheral heavy ion collisions. We first review the Feynman graph approach to pair production in relativistic heavy ion collisions. The lowest order (Born approximation) cross section was given by Landau and Lifshitz [6] and Racah [7] in the thirties of the past century. In contrast to the photoproduction on a nucleus one has a well-defined impact parameter in heavy ion collisions and impact-parameter dependent probabilities have been studied as well. Higher order effects were studied in the
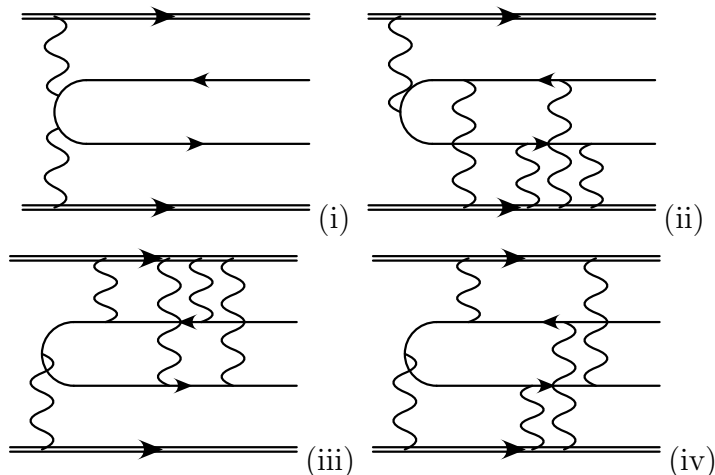
Fig. 3. e^+e^- pair production is classified by the number of photons attached to each ion. We distinguish for classes (i) $n = n' = 1$ (ii) $n = 1$, $n' > 1$ (iii) $n > 1$, $n' = 1$ and (iv) $n > 1$, $n' > 1$.

last decades, mainly by the russian schools. We note here that due to the high mass of the projectile bremsstrahlung pair production is negligible at the high energies, as explained, e.g., in [26], see also [28]. Bremsstrahlung pair production is relevant for lower beam energies, where the (timelike) bremsstrahlungsphoton is converted to an e^+e^- pair.

As we will see in the following we have an important classification of the terms: We denote the number of photons attached to nucleus 1 by n, to nucleus 2 by n' and distinguish four classes, see Fig. 3:
(i) $n = 1$ and $n' = 1$
This is the lowest order case as treated by Landau and Lifshitz [6] and Racah [7]. The cross section increases with the Lorentz factor γ like $(\log \gamma)^3$ and is the dominant term at high energies.
(ii) $n = 1$ and $n' > 1$
(iii) $n > 1$ and $n' = 1$
These terms are the main correction and well understood as we will show. The problem is essentially the same as the one for the Bethe-Heitler process, and it is solved in an analogous way.

The case, which is specific to heavy ion collisions and which contains all the problems is the last one:
(iv) $n > 1$ and $n' > 1$
This case cannot be considered to be solved, but at least it is reassuring that one can show that it is only a small contribution to the cross section. This classification is directly evident in the Feynman diagram approach of Sec. 3, but it also plays the major role in the approaches of Sec. 5. When the ion velocity decreases or for small impact parameter the Feynman diagrams of class (iv) will become more important. So collisions at intermediate and small

energies become increasingly difficult to treat theoretically. Molecular orbital approaches will then become relevant. This is quite analogous to the situation in atomic physics for the excitation of atoms by ions in ion-atom collisions. This is an interesting topic but it is outside the scope of this review.

In Sec. 4 an analytical solution to the (one-particle) time dependent two-center Dirac equation in the high energy limit is discussed. The authors of [29,30,31,32] were led to the (erroneous) conclusion that the cross section corresponding to the exact solution is the same as the cross section in the Born approximation. But this is in obvious contradiction to the special case of the Bethe-Maximon corrections to the Bethe-Heitler formula. There are two aspects in this work: one is related to the interpretation of the one-particle Dirac equation to the corresponding (many-body) Feynman diagrams describing pair production. We will show how the two can be related, see, e.g. [33,34]. The other aspect has to do with the proper regularization of the expression, which was used by [29,31,32,35] in the high energy (sudden) limit.

In Sec. 5 we discuss the work of Ivanov, Schiller and Serbo [36] and Lee and Milstein [37]. The latter work is based on the analytical solution of the Dirac equation in Sec. 4. In Sec. 6 we discuss some aspects of class (iv): two- or more photons emerge from either nucleus: in addition to the 'Coulomb corrections', which are small, there is a new genuine higher order effect: the multiple pair production in a single collision. Another higher order effect (belonging essentially to classes (ii) and (iii)) is bound-free pair production: the electromagnetic interaction of the ion (to all orders) with the electron leads to a bound state (K-,L-shell,...capture). This is a small but interesting fraction of the total pair production, the cross section scales only with $\log(\gamma)$, instead of $(\log(\gamma))^3$ for free pairs. In Sec. 7 we make some remarks about the transition from the non-perturbative slow to the perturbative fast collisions. This is a difficult question. We discuss especially the results of [15]. An interpolation between the two limits is achieved analytically for the case of spatially constant electric fields. In Sec. 8 we give a comparison of theory to experiment: in the last five years since our previous review [18] RHIC has come into operation. We compare the experimental results of STAR on e^+e^- pair production in UPC [38] to lowest order QED calculations and discuss the results of bound-free pair production at RHIC. Accelerator physicists are anxious to test the theory of bound-free pair production because this process is crucial for the operation of the forthcoming LHC(Pb-Pb). The bound-free capture process will be the ultimate limit for the Pb-Pb luminosity. Conclusions and an outlook are given in Sec. 9.

Throughout this review we use $\hbar = c = 1$ and $\alpha = e^2$, unless it seems of some pedagogical value to include these constants explicitly. We also assume relativistic high energy collisions, which are characterized by $\gamma \gg 1$. We assume that even $\log(\gamma) \gg 1$. This is well fulfilled for RHIC and LHC conditions, less

so for AGS and SPS energies.

2 Lepton pair production by a high energy photon in the strong Coulomb field of a heavy nucleus

In this chapter we recall the well known theoretical treatment of the Bethe-Heitler process, the e^+e^- pair production by a photon in the Coulomb field of a nucleus. This is simpler than the problem of pair production in the field of two nuclei, but shows already many of the important aspects of the nucleus-nucleus case. It corresponds to the cases (i), (ii) and (iii) (see Sec. 1), where only one photon is attached to one of the nuclei. Case (iv) is the one, which is specific to the nucleus-nucleus problem.

The Born approximation result (case (i)) is derived in textbooks using the well established tools of QED, see e.g. [26]. The celebrated Bethe-Heitler result for the total cross section of the process

$$\gamma + Z \rightarrow e^+ + e^- + Z \tag{6}$$

in the case of no screening is given in the high energy limit by

$$\sigma_1 = \frac{28}{9} \frac{\alpha^3 Z^2}{m^2} (\log \frac{2\omega}{m} - \frac{109}{42}), \tag{7}$$

where the photon energy is denoted by ω. The Coulomb field of the nucleus is treated as an external field. It is a characteristic feature that the cross section rises logarithmically with the photon energy. Screening due to the atomic electrons leads to a constant cross section for high energies. This screening effect is of little interest for us here, as we are mainly interested in the case of bare ions at the colliders.

The higher order effects in pair production at high photon energies and also for large energies of electron and positron compared to their rest mass, were studied by Bethe, Maximon and Davies [24,25].

Their results are also described in detail in many textbooks (see especially [26]). For the derivation of the cross section these authors used Sommmerfeld-Maue wave functions for the electron and the positron, respectively. These wave functions are approximate solutions of the Dirac equation in the nuclear Coulomb field valid for high energies and small scattering angles. Thus they include, in a certain way, higher order effects up to all orders. They are given for the electron with energy ε_- and momentum $\overrightarrow{p}_-$ by:

$$\psi_{\varepsilon_-p_-}^{(-)} = \frac{N_-}{\sqrt{2\varepsilon_-}} e^{i\overrightarrow{p}_- \cdot \overrightarrow{r}} (1 - i\frac{\overrightarrow{\alpha} \cdot \nabla}{2\varepsilon_-}) F(-iZ\alpha, 1, -i(p_- r + \overrightarrow{p}_- \cdot \overrightarrow{r})) u(p_-) \tag{8}$$

with the normalization

$$N_- = \exp(\frac{\pi}{2}Z\alpha)\Gamma(1 + iZ\alpha) \tag{9}$$

depending on the Γ-function and the confluent hypergeometric function F. The Dirac spinor for the electron in the free case is given by u and $\overrightarrow{\alpha}$ are the Dirac matrices.

Similarly the wave function for the positron is given by:

$$\psi^{(+)}_{-\varepsilon_+ p_+} = \frac{N_+}{\sqrt{2\varepsilon_+}} e^{-i\overrightarrow{p}_+ \cdot \overrightarrow{r}} (1 + i\frac{\overrightarrow{\alpha} \cdot \nabla}{2\varepsilon_+}) F(-iZ\alpha, 1, i(p_+ r + \overrightarrow{p}_+ \cdot \overrightarrow{r})) u(p_+) \tag{10}$$

with

$$N_+ = \exp(-\frac{\pi}{2}Z\alpha)\Gamma(1 - iZ\alpha). \tag{11}$$

Inserting these wave functions into the standard matrix element, differential and total cross section can be calculated analytically, leading (after neglecting some small terms in the high energy limit) to the expression for the total cross section:

$$\sigma_1 = \frac{28}{9}\frac{\alpha^3 Z^2}{m^2}(\log\frac{2\omega}{m} - \frac{109}{42} - f(Z\alpha)), \tag{12}$$

where the Bethe-Heitler cross section, see Eq. (7) above is now modified by a term containing the function $f(\alpha Z)$. It is defined by:

$$f(Z\alpha) = \gamma_E + Re\Psi(1 + iZ\alpha) = (Z\alpha)^2 \sum_{n=1}^{\infty} \frac{1}{n(n^2 + (Z\alpha)^2)}, \tag{13}$$

where $\gamma_E = 0.57721...$ is the Euler-Mascheroni constant [39] and Ψ the logarithmic derivative of the Γ-function. Note that in this way higher order effects are established without making use of perturbative QED. In fact, Feynman graphs up to infinite order are effectively summed up by the use of these Sommerfeld-Maue wave functions.

It is very interesting to see that the same results can also be derived directly (among other things) by the standard method of summing up all Feynman graphs [27], see Fig. 4. This establishes the equivalence between the standard higher order QED approach and the calculations using Sommerfeld-Maue wave functions. This is very important for our problem below: As discussed in the
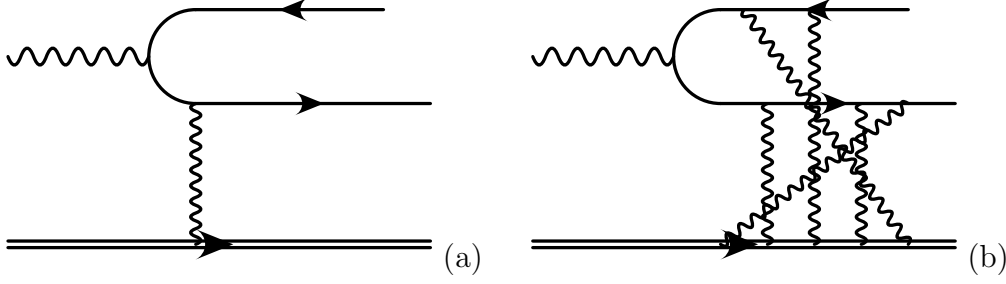
Fig. 4. (a) Pair production in photon-nucleus scattering in lowest order of $Z\alpha$. (b) Higher order term. These terms are summed up in the Bethe-Maximon theory using the Sommerfeld-Maue wave functions, or by summing the Feynman graphs according to the approach of [27].

following chapters, there are again the Feynman diagram approaches to the nucleus-nucleus problem, and the 'Sommerfeld-Maue type' of approaches.

In the following, we very briefly describe the work of Ivanov and Melnikov [27]. A typical type of Feynman graphs to be calculated is shown in Fig.4, (which is Fig. 1 of [27]). For $N = 1$ this corresponds to the Born approximation: the e^+e^- pair is produced by the collision of a real photon (which can also be virtual in [27]) and a virtual photon coming from the nuclear Coulomb field.

Many steps are needed to sum up the Feynman graphs in the high energy limit. We sketch some of the important points: The basic kinematics is $p_1 + p_2 = p_1^{'} + q_1 + q_2$ and it is convenient to regard the nucleus as a light particle with mass m and charge Z. We assume $2p_1 \cdot p_2 \equiv s \gg m^2, Q^2$. We denote $p_1^2 = -Q^2$; for a real photon we have $Q^2 = 0$. There are two important scales for the square of the transverse part of the transferred momentum $q \equiv q_1 + q_2 - p_1$: $\vec{q}^{\,2} \sim m^2, Q^2$ and $\vec{q}^{\,2} \sim m^4/s, Q^4/s$. The second low momentum transfer region is only important for the case where one photon is exchanged, it is responsible for the logarithmic rise of the cross section. For the case of more than one photon exchange with the nucleus the first region is the dominant one.

For the high energy limit considered in [27] the so-called Sudakov variables are used as the appropriate variables. They are light-like vector $\tilde{p}_1$ and $\tilde{p}_2$, which are pointing almost in the direction of p_1 and p_2. They are given by

$$\tilde{p}_1 = p_1 + \frac{Q^2}{s}p_2, \qquad \tilde{p}_2 = p_2 - \frac{m^2}{s}p_1. \tag{14}$$

These Sudakov variables can also be related to the so-called light-cone variables. The use of these variables allows to express the four-dimensional loop integrals occuring in the calculation of the Feynman diagrams in terms of the transverse momentum only. The transverse momentum integrals themselves are expressed in coordinate (impact-parameter)space and the high energy amplitude contains the so-called impact factors. These are scalar and vector struc-

ture quantities for the exchange of N-photons. Using recursion relations and other tricks to which we can only refer to the original paper [27] the authors are able to sum them.

The full result for the cross section for the pair production due to a virtual photon γ^* and where all the graphs with $N = 1$ to $N = \infty$ are summed is given in Sec. IV B of [27]. For a real incident photon the result was found to be identical to the one obtained previously by using the Sommerfeld-Maue wave functions. The methods of [27] can also be applied to the relativistic heavy ion case, which is the subject of the next section.

Just as in [27], we are especially interested in the high energy limit, but it is also of more general interest to study corrections in $\frac{1}{\omega}$. For this question we refer to Ref. [40].

We note that the theoretical results in the high energy small scattering angle limit are symmetric with respect to the exchange of e^+ and e^-. It is certainly not the case for bound-free pair production, a process to be discussed in Sec. 6, see [41,42]. We also mention without further discussion that another asymmetry was introduced by Brodsky and Gillespie [43] in their second order Born treatment of large angle e^+e^- pair production.

3 Lepton pair production in relativistic heavy-ion collisions using Feynman diagrams

In this paragraph we want to briefly review the work on e^+e^- pair production in relativistic heavy ion collisions based on the summation of Feynman graphs in the high energy limit. The problem is formulated in [44]. The process to be studied is

$$A(p_1) + B(p_2) \rightarrow e^+(q_+) + e^-(q_-) + A(p'_1) + B(p'_2), \tag{15}$$

where the corresponding four-momenta are given in the brackets.

In the paper [44] the first terms in the amplitude of e^+e^- pair production in the Coulomb field of two relativistic heavy ions are calculated. The Sudakov technique is used which simplifies the calculations at high energies, see Sec. 2. In lowest order in α (corresponding to class (i), see Fig 3) the classic result of Racah is obtained

$$\sigma = \frac{\alpha^4 Z_1^2 Z_2^2}{\pi m^2} \frac{28}{27}(L^3 - 2.2L^2 + 3.84L - 1.636), \tag{16}$$

where $L \equiv \ln(\gamma_1\gamma_2) = \ln(\gamma^2)$ for symmetric collisions. For details we refer to reference [44]. Also further references are given there, which actually give the steps needed to derive the Racah formula by their methods.

Next they consider Coulomb corrections. The first correction corresponds to the case where one nucleus emits one and the other nucleus emits two photons $(n = 1, n' = 2)$, corresponding to the lowest order diagram of class (ii). This contributes to the Coulomb corrections with the pair produced in an C-odd state. Altogether six Feynman diagrams contribute to this amplitude.

The first C-even correction involves graphs where $n = 1, n' = 3$ (belonging again to class (iii)) and $n = 2, n' = 2$ (the lowest order diagram contributing to class (iv)). Whereas the former case proved to be tractable analytically, obstacles were found for the second case. An explicit calculation of the $n = 2, n' = 2$ case is reported in [45]. Their result suggests that the familiar eikonalization of Coulomb distortions breaks down for the oppositely moving centers.

Lepton pair production in relativistic ion collisions to all orders in $Z\alpha$ with logarithmic accuracy is studied in [46]. The amplitude is separated into the four terms

$$M = M_{(i)} + M_{(ii)} + M_{(iii)} + M_{(iv)} \tag{17}$$

corresponding to the four different classes defined in the introduction. Different terms in the absolute square of the amplitudes can then be classified according to their energy dependence, i.e. by their dependence on different powers of the large logarithm $L = \ln(\gamma_1\gamma_2) = \ln(\gamma^2)$. The absolute square of the Born amplitude $|M_{(i)}|^2$ leads to the famous rise of the cross section with L^3. It should be noted that the Racah formula (see Eq. (16)) contains also terms proportional to L^2 and L. As discussed in [44] the next powers of L come from the absolute square of $M_{(ii)}$ and $M_{(iii)}$ and their interference with the Born amplitude $M_{(i)}$. The leading term of their result coincides with the one found by other methods, which will be described below. Their result for the Coulomb corrections in order L^2 is of the 'Bethe-Maximon type':

$$\sigma_c = \frac{28\alpha^4 Z_1^2 Z_2^2}{9\pi m^2}(f(Z_1\alpha)f(Z_2\alpha)L^2 + O(L)), \tag{18}$$

where $f(Z\alpha)$ was defined in Eq. (13).

A direct manifestation of strong fields is multiple pair production. Early work on this subject started with the observation that the impact parameter dependent total pair production probability calculated in lowest order perturbation theory is larger than one, i.e. $P^{(1)}(b) > 1$. More on multiple pair production will be given in Sec. 6. The analysis of [47] fits in naturally within the approach to study Feynman graphs in the high energy limit. The general Feynman diagram is shown in Fig. 5. It has N_s light-by-light (LBL) blocks N_e photon exchanges between the ions Z_1 and Z_2 (not present in an external field approach) and N pair production processes. Coulomb corrections are neglected. They assume $Z_{1,2} \gg 1$, $Z_1\alpha \sim Z_2\alpha < 1$ and $Z_1 Z_2\alpha > 1$. The probability of N pair production is shown to obey a Poisson distribution.

In [48] a new approach to lepton pair production in the Coulomb field of two relativistic nuclei was developed. It was shown that for certain sums of finite terms of the Watson series cancellations lead to infrared stability of the amplitude (i.e. the result does not depend on a screening radius of the Coulomb field).
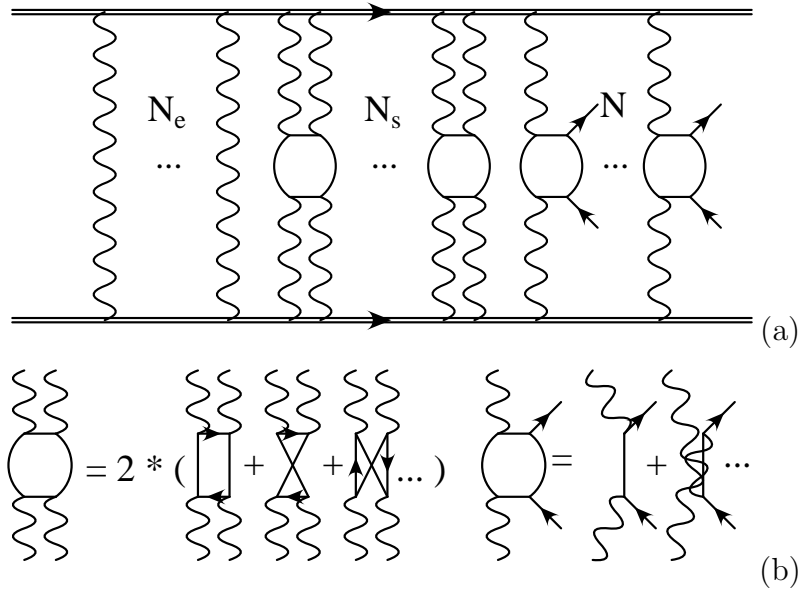
Fig. 5. A general diagram for the process of N-pair production in ultraperipheral nucleus-nucleus collisions is shown. It contains N_e photon exchanges between the nuclei, N_s light-by-light scattering blocks and N e^+e^- pair production diagrams. The symbols for light-by-light scattering blocks and pair production diagrams are given in terms of the Feynman graphs in Fig. (b).

4 Exact solution of the one-particle Dirac equation in the ultrarelativistic limit and what one can conclude from that

An interesting topic is the solution of the (single-particle) Dirac equation for two countermoving ions and how this relates to the process of pair production. This was strongly triggered by the observation, that in the limit of ultrarelativistic nuclei and using an appropriate gauge, the expression for the electromagnetic interaction simplifies and the Dirac equation can be solved analytically in a closed form [49].

Before we discuss this specific solution of the Dirac equation, it is useful to remember that e^+e^- pair production is a problem in relativistic quantum field theory. It is inherently a many-particle theory from the beginning, where particles can be created and destroyed. In contrast to this situation the familiar problem of ionization of an atom by a non-relativistic heavy projectile can indeed be dealt with by the time-dependent Schrödinger equation: the atomic electron (say in a hydrogen atom) is described by a Hamiltonian $H_0 = T + e^2/r$. The classical motion of the projectile causes a time-dependent perturbation $V(t)$ and the problem is to solve the time-dependent Schrödinger equation for the wave function Φ of the electron

$$i\frac{\partial \Phi}{\partial t} = (H_0 + V(t))\Phi(t). \tag{19}$$

This equation can be solved by a number of well-established methods like perturbation theory, see e.g. [50]. For special cases, like the harmonic oscillator, there are also full analytical solutions. Alternatively, one can solve numerically the Schrödinger equation for the wave function $\Phi(t)$ and project on specific asymptotic states in order to determine the cross-section for transitions to these final states.

In the case of e^+e^- pair production Eq. (19) has a different meaning: Φ is now a state vector, the term $V(t) = j_\mu A_\mu$ is the interaction of the time-dependent (external) field $A_\mu(t)$ with the electromagnetic current operator $j_\mu = \bar{\Psi}\gamma_\mu\Psi$. This current can be written in terms of electron and positron creation and annihilation operators. One gets different terms describing electron and positron scattering, as well as, e^+e^- pair production and annihilation. This problem is solved by the Dyson expansion (see, e.g., [26] or other textbooks on Quantum field theory). This approach then leads to amplitudes for e^+e^- pair production not only for single pair production, but for $N = 0, 1, 2, \ldots$ pair production. Multiple pair production will be discussed later in Sec. 6. Here we want to discuss only the relation between a solution of the Dirac equation and the pair production process. That there is a problem with the interpretation of the one-body Dirac equation can already be seen in the discussion of the free

Dirac propagator, see e.g. Chap. 2-5 of [12]. The solution of the (free) Dirac equation (with $V(t) = 0$) can be written as

$$\Psi(t_2, \vec{x}_2) = \int d^3 x_1 K(t_2, \vec{x}_2; t_1, \vec{x}_1) \gamma_0 \Psi(t_1, \vec{x}_1), \tag{20}$$

where $K(x_2, x_1)$ is the retarded kernel. However, as is remarked on p. 90 of [12], the hole theory suggests the introduction of a different propagator, the Feynman propagator. It appears in a natural way in the quantized field theory.

In our case here, that is, for the interaction with only an external field we can find at least a relation between the two pictures, which we quickly want to sketch here. For further details we refer to [33,51]. Only for certain processes one can neglect the many-particle aspect. This is for example the case for photoproduction, where the interaction with only one photon and a static Coulomb field leads to only one electron lifted from the negative sea to the positive continuum.

Baltz, Gelis, McLerran and Peshier discuss the meaning of the exact solution of the Dirac equation in Ref. [30]. They make a valid point: the interpretation of the solution of the one-body Dirac equation is not straightforward. They show that the total cross-section obtained in this approach does not correspond the exclusive cross-section to produce exactly one pair, but to one where multiple pair production cross section are also included (each weighted by the number of particles produced). This is rederived in a very straightforward manner in [33].

The relation between the two approaches can be found in the following way, see [33] or [2,52] for details. The S-matrix of the Dirac equation relates the annihilation operators for the electrons b and creation operators for positrons d, respectively, in the initial (i) and final (f) state in the following way:

$$\begin{pmatrix} b^f \\ d^{f+} \end{pmatrix} = S \begin{pmatrix} b^i \\ d^{i+} \end{pmatrix} = \begin{pmatrix} S_{++} & S_{+-} \\ S_{-+} & S_{--} \end{pmatrix} \begin{pmatrix} b^i \\ d^{i+} \end{pmatrix}. \tag{21}$$

Here the indices $+$ and $-$ refer to the positive or negative energy, that is S_{-+} is the transition from a positive to a negative energy state. It is this matrix S that is calculated by solving the Dirac equation.

For the Feynman boundary condition one prescribes the initial electron and the final positron (following the picture of Feynman that the positrons are electrons traveling back in time) and solves the field equations to get the final electron and initial positron states. For single pair production we have one positron in the final state and calculate those processes leading to an electron

in the final state. Therefore we need to rewrite the relation in Eq. (21) as one between the b^i and d^{f+} on the one and the b^f and d^{i+} on the other side. One gets

$$b^f = (S_{++} - S_{-+}S_{--}^{-1}S_{-+})b^i + S_{+-}S_{--}^{-1}d^{f+}. \tag{22}$$

The first term is of interest for electron scattering, whereas the second term is the one we are interested in. In addition we need to add the vacuum-vacuum transition amplitude C, see Sec. 6 below, to get for the matrix element for the single pair production process

$$M_{kl} = \langle 0|b_k^f d_l^f|0\rangle = C(S_{+-}S_{--}^{-1})_{kl}. \tag{23}$$

Having a complete solution of the Dirac equation one can now in principle invert S_{--} (the amplitude for the scattering of positrons to positrons) in order to get the correct single-pair production amplitude.

In the papers of Segev and Wells [31,32], Baltz and McLerran [29] and Eichmann, Reinhardt, Schramm and Greiner [35] a remarkable analytic solution of the (one-body) Dirac equation is found. It was shown subsequently by Lee and Milstein how to regularize this expression and to find a useful solution for the Coulomb correction problem (see the next Sec. 5). By a suitable gauge transformation [29] the potential created by the counter-moving ultrarelativistic ions can be written as

$$V(\rho, z, t) = -\theta(t - z)\vec{\alpha} \cdot \nabla\Lambda^-(\rho) - \theta(t + z)\vec{\alpha} \cdot \nabla\Lambda^+(\rho), \tag{24}$$

where

$$\Lambda^{\pm}(\rho) = -Z\alpha \ln \frac{(\vec{\rho} \pm \vec{b}/2)^2}{(b/2)^2}. \tag{25}$$

Except at $x^{\pm} \equiv \frac{1}{\sqrt{2}}(t \pm z)$ the electron or positron propagates as a free particle. As is remarked in [29], to construct the propagator for the electron, one needs to solve a boundary value problem with free propagation everywhere except at the surfaces of discontinuity at the light cone $x^{\pm} = 0$, see Fig. 6. The final result is their Eq. (51). We do not give it here but refer to the next section, where the work in [53] and [54] is discussed. There one starts from their formula Eq. (24), which is now contained in Eqs. (30)–(33) of Sec. 5 and show how to regularize this result correctly.
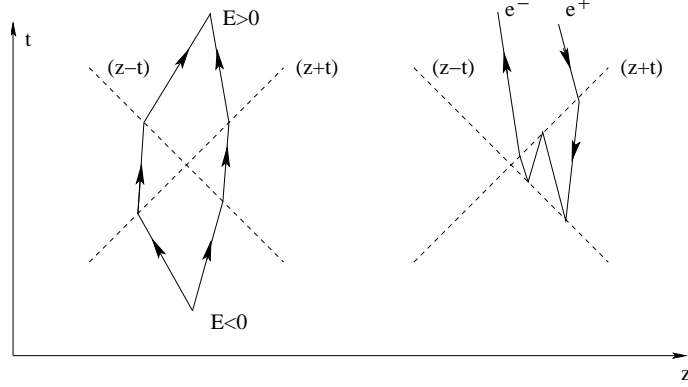
20

Fig. 6. The special structure of the electromagnetic interaction can be seen in this t-z plot. Due to the Lorentz contraction, the electromagnetic fields are localized in two sheets corresponding to $z = \pm t$. In the 'retarded' or 'Dirac sea' approach (left), an electron with negative energy comes from $t = -\infty$, crosses the field of each ion only once before leaving as an electron with positive energy. In the 'Feynman' approach (right), the positron comes from $t = +\infty$ and can go forward and backward in time interacting a number of times with the ions.

5 Coulomb corrections for the heavy ion case, based on the Bethe-Maximon approach

In the last section the exact solution of the one-particle Dirac equation in the high energy limit was discussed. Using the eikonal/sudden approximation at high energies it was claimed in several publications that Coulomb corrections are not present. This claim must be wrong, since one has to reproduce the Bethe-Maximon results for photoproduction, see Sec. 2 in the limit where the charge of one nucleus Z_1 is small, i.e. $Z_1\alpha \ll 1$. In Sec. 3 we dealt with pair production in the "usual" approach of QED, that is the perturbative calculation and summation of Feynman diagrams. We saw that in the papers which we briefly reviewed very powerful techniques could be used to simplify the calculations at high energies. Also various terms could be summed analytically. In the end an agreement with the Bethe-Maximon results was found. Yet, people not so familiar with these techniques might feel a little lost and other approaches (still for the high energy case) might be preferable. This is the subject of the present section.

Before starting it may be mentioned that in Ref. [20] it was already realized that there was a problem with higher order Coulomb corrections, see Chap. 7.3 there. There are corrections of the Bethe-Maximon type (class (ii) and (iii) in our notation) and corrections due to class (iv) (with $n, n' > 1$). An 'interpolating' function $\bar{f}(Z_1, Z_2)$ was conjectured in [20] (see Eq. (7.3.7)), in order to take care of these corrections but the question remained inconclusive. The convincing answer for the Coulomb corrections was first given in Ref. [36].

5.1 *Coulomb corrections in the equivalent photon approximation: the approach of Ivanov, Serbo and Schiller*

Let us now briefly review the approach of Ref. [36]. These authors start with a classification of the pair production amplitudes $M_{nn'}$ according to the number of photon lines attached to each ion, that is, the classification introduced in Sec. 1. The sum of the amplitudes is written as $\sum_{nn'} M_{nn'} = M_{Born} + M_1 + \tilde{M}_1 + M_2$, corresponding to $M_{(i)} + M_{(ii)} + M_{(iii)} + M_{(iv)}$ in our notation. The Born amplitude contains the one-photon exchange with each nucleus (class (i)), the amplitudes M_1 and $\tilde{M}_1$ correspond to classes (ii) and (iii), M_2 are the processes of class (iv). In their Eq. (8) the total cross section is classified according to

$$\sigma = \sigma_{Born} + \sigma_1 + \tilde{\sigma}_1 + \sigma_2, \tag{26}$$

where

$$d\sigma_{Born} \sim |M_{Born}|^2 = |M_{(i)}|^2 \tag{27}$$

and

$$d\sigma_1 \sim 2Re(M_{Born}M_1^*) + |M_1|^2 = 2Re(M_{(i)}M_{(ii)}^*) + |M_{(ii)}|^2 \tag{28}$$

etc. Now the authors estimate the leading logarithms $L \equiv \ln(\gamma_1\gamma_2) = \ln(\gamma^2)$ (see Eq. (16) in Sec. 3) appearing in the cross sections σ_i. Due to the integration over the transferred momenta there are two large logarithms L in $\sigma_{Born} \sim L^2$ and one large logarithm L for $\sigma_1 \sim L$ and $\tilde{\sigma}_1 \sim L$. There is no large logarithm for $\sigma_2 \sim L^0$. (Eventually, there will be another logarithm due to the integration over the energy of the e^+e^- pair.) Therefore this last (and most troublesome) term can be neglected, to a good accuracy, in the high energy limit when calculating the cross section. Please note that this argument is true for the cross section. As we will discuss below it does not hold for impact parameter dependent probabilities, especially for small impact parameters b.

In order to study the higher order effects, the method of *equivalent photons* is used. Thus the higher order effects are reduced to a study of the higher order effects in the photoproduction (by real photons). These corrections are well known, see Sec. 2, and given in Eqs. (10)–(13) of Ref. [36]. Their final result is the expression Eqs. (24)–(27) for σ_1, and a corresponding one for $\tilde{\sigma}_1$. As discussed above, it is proportional to L^2. Further, it is estimated that $\sigma_2/\sigma_{Born} \sim (Z\alpha)^2/L^2$. Therefore this last class of processes will give a contribution so small that one can neglect this contribution for practical purposes. In order to see these effects either a very good accuracy would be needed, or one should find a way to increase their relative importance. One possibility to enhance the importance of small impact parameters is discussed in Sec. 8. Their final result (Eq. (27)) for the Coulomb correction is then

$$\sigma_{Coul} \approx \sigma_1 + \tilde{\sigma}_1 = -\frac{56}{9}\sigma_0 f(Z)L^2, \tag{29}$$

where f is given in Eq. (13) in Sec. 2 and $\sigma_0 = \frac{\alpha^4 Z_1^2 Z_2^2}{\pi m^2}$.

It is also noted that the large transverse momenta $\vec{p}^2 \gg m^2$ give a negligible contribution to the total cross section, but the experiments of STAR at RHIC (see Sec. 8 below) are just in this region, since one needs the high transverse momentum to detect the electrons.

As shown above we know that there are indeed Coulomb corrections. They are predominantly given by the Coulomb corrections which are present in the photonuclear case.

In order to see the Coulomb corrections in the exact solution of the Dirac equation, we need to study in more detail the regularization that is needed in the sudden limit. In this limit all longitudinal momentum transfers are neglected. In this case the cross section would diverge, as large impact parameters contribute to arbitrary large values. Therefore a regularization of the result is needed. This is done in a certain way, by adding a longitudinal component to the final result in [29]. Another approach is to calculate only the deviation of the full results from the Born result, as it is only the Born result, which leads to a divergence. In [53,54] it is shown how to obtain reasonable results from the expression of Segev and Wells [55] and Baltz and McLerran [29]. The problem of the slowly decaying Coulomb potential is solved by introducing a screening of the Coulomb potential. Eventually the screening parameter is extended to infinity. The procedure of [54] and [53] is a nice example of the power of analytic methods. In order to outline their reasoning we would like to repeat some of the key steps of this work. For details we have to refer to their work.

The authors of [53] start from an expression derived by Segev and Wells [55] and Baltz and McLerran [29] for the total pair production cross section, see their Eq. (1)

$$dσ = \frac{m^2 d^3p\, d^3q}{(2π)^6 ε_p ε_q} \int \frac{d^2k}{(2π)^2} |F_B(\vec{k})|^2 |F_A(\vec{q}_\perp + \vec{p}_\perp - \vec{k})|^2 |M(\vec{k})|^2. \tag{30}$$

Here $\vec{k}$ is a vector lying in the plane transverse to the momenta of the ion(s). The amplitude M is given by

$$M(\vec{k}) = \bar{u}(p)[\frac{\vec{α} \cdot (\vec{k} - \vec{p}_\perp) + γ_0 m}{-p_+ q_- - (\vec{k} - \vec{p}_\perp)^2 - m^2}γ_-$$

$$+ \frac{-\vec{α} \cdot (\vec{k} - \vec{q}_\perp) + γ_0 m}{-p_- q_+ - (\vec{k} - \vec{q}_\perp)^2 - m^2}γ_+]u(-q), \tag{31}$$

where $\vec{p}$ and $ε_p$ ($\vec{q}$ and $ε_q$) are momentum and energy of the electron (positron), $u(p)$ and $u(-q)$ are positive and negative energy Dirac spinors, $\vec{α} = γ^0\vec{γ}$, $γ_\pm \equiv γ^0 \pm γ^z$, $γ^μ$ are the Dirac matrices. We use light-cone variables $p_\pm = ε_p \pm p^z$ and
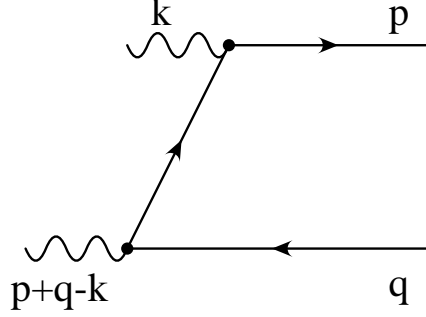
24

Fig. 7. One of the two lowest order diagrams for the pair production from two (virtual) photons with momenta k and $p + q - k$.

$q_\pm = \epsilon_q \pm q^z$. The function $F(\Delta)$ describes the interaction with the Coulomb field of one of the ions. It is proportional to the electron eikonal scattering amplitude for one of the potentials $V(r)$:

$$F(\Delta) = \int d^2\rho \exp(-i\vec{\rho} \cdot \vec{\Delta})(\exp(-i\chi(\rho)) - 1), \qquad (32)$$

where

$$\chi(\rho) = \int\limits_{-\infty}^{+\infty} dz V(\rho, z). \qquad (33)$$

For an unscreened Coulomb potential $V(r) = -Z\alpha/r$ the integral for the Glauber phase $\chi(\rho)$ becomes divergent and a regularization is required. One can choose, e.g., $V = -Z\alpha \exp(-r/a)/r$, i.e., the Coulomb potential is smoothly cut off at a radius a. Eventually, the radius a will tend to ∞. It is shown in [53,54] that the result is independent of the particular method used, as long as $V(r) \to -Z\alpha/r$ for $r \to 0$.

Using Eq. (9.6.23) of Ref. [56] and the substitution $dz = rdr/\sqrt{r^2 - \rho^2}$ we find that $\chi(\rho) = \int dz V(b, z) = -2Z\alpha K_0(\rho/a)$. Using the following well-known representation of the Bessel function (see e.g. [56])

$$J_0(z) = \frac{1}{2\pi} \int\limits_0^{2\pi} e^{iz \cos\phi} d\phi, \qquad (34)$$

one finds Eq. (11) of [54]:

$$F(\Delta) = 2\pi \int\limits_0^\infty d\rho\rho J_0(\rho\Delta)(\exp 2iZ\alpha K_0(\rho/a) - 1) \qquad (35)$$

Let us now take the limit $a \to \infty$ for a fixed $\Delta \neq 0$. For $\rho/a \ll 1$ we have $K_0 \sim \ln(\rho/a)$ and we get an integral of the type

$$F(\Delta) \approx 2\pi \lim_{a \to \infty} \int_0^\infty d\rho \rho J_0(\rho\Delta)(\exp 2iZ\alpha \ln(\rho/a) - 1). \tag{36}$$

This is a well-known generalization of the Bethe integral and one obtains

$$F = i\pi Z\alpha \frac{\Gamma(1 - iZ\alpha)}{\Gamma(1 + iZ\alpha)} \left(\frac{4}{\Delta^2}\right)^{1 - iZ\alpha}. \tag{37}$$

Up to an overall constant phase, we see that the effect of the higher order Coulomb interaction consists of a change of the photon propagator $1/\Delta^2$ to $1/(\Delta^2)^{1 - iZ\alpha}$. This result was already found in [29]. Taking the square of $F(\Delta)$ one gets

$$|F(\Delta)|^2 \sim \left|\frac{1}{(\Delta^2)^{1 - iZ\alpha}}\right|^2 = \frac{1}{\Delta^4}, \tag{38}$$

independent of $Z\alpha$, which is the reason why the absence of Coulomb corrections was found in their case. But one should keep in mind, that Δ is the transverse part of the momentum transfer from the ions only. In [53,54] a recipe is given that is used in order to obtain the "correct Coulomb correction". It is necessary to do the integration over k first in Eq. (30) using the function $F(k)$ with the regularized phase and then to remove the regularization only afterwards.

Before the Coulomb correction to electron positron pair production itself is studied in refs. [53,54] these authors studied the integral

$$G = \int \frac{d^2k}{(2\pi)^2} k^2 (|F(\vec{k})|^2 - |F^0(\vec{k})|^2), \tag{39}$$

where $F^0(\Delta) = -i \int d^2\vec{\rho} \exp(-i\vec{\Delta} \cdot \vec{\rho})\chi(\rho)$ corresponds to the Born expression.

We integrate $F(\Delta)$ of Eq. (35) by parts over ρ to obtain:

$$F(\Delta) = \frac{2\pi i}{\Delta} \int_0^\infty d\rho \rho J_1(\Delta\rho)\chi'(\rho) \exp(-i\chi(\rho)). \tag{40}$$

In order to obtain this result recursion relations for the Bessel functions are used (see Eq. (9.1.27) of [56]). The function $F^0(k)$ can be obtained from

Eq. (40) by omitting the exponent in the integrand. Now the expression for G reads

$$G = 2\pi \int\limits_0^\infty dk\, k \int\limits_0^\infty \int\limits_0^\infty d\rho_1 d\rho_2 \rho_1 \rho_2 J_1(k\rho_1) J_1(k\rho_2) \chi'(\rho_1) \chi'(\rho_2)$$
$$\times (\exp(-i\chi(\rho_1) + i\chi(\rho_2)) - 1). \tag{41}$$

A naive interchange of the order of integration would lead to $G = 0$, since due to the orthogonality relation for the Bessel functions the integration over k leads to a term proportional to $\delta(\rho_1 - \rho_2)$.

Instead the authors of Ref. [53] proceed in another way: they integrate k up to a finite fixed value Q, instead of ∞. According to Eq. (11.3.30) of Ref. [56] (for $\mu = \nu = 0$) this gives their Eq. (7).

The final result for G is then found to be

$$G = -8\pi(Z\alpha)^2 f(Z\alpha), \tag{42}$$

where, again, we encounter the ubiquitous function $f(Z\alpha)$ of Eq. (13) above.

Now we proceed to the Coulomb correction itself. The Coulomb corrections are defined in the usual way discussed above as the difference of the full result to the Born result. One obtains three terms, see Eqs. (7) and (8) of [54]. In [53,54] it is argued that the main contribution to the integrals comes from the region of small k. Accordingly, the matrix-element M of Eq. (31), is expanded as

$$M = k_i k_j' M_{ij}, \tag{43}$$

where $k' = q + p - k$. In [54] $|M_{ij}|^2$ is then calculated explicitly. This decomposition into three terms corresponds to the decomposition already discussed above in Eq. (26):

$$\sigma = \sigma_{Born} + \sigma_A^c + \sigma_B^c + \sigma_{AB}^c = \sigma_{Born} + \sigma_1 + \tilde\sigma_1 + \sigma_2. \tag{44}$$

We have $\sigma_{Born} \sim L_A L_B$, $\sigma_A^c \sim G_A L_B$, $\sigma_B^c \sim L_A G_B$, and $\sigma_{AB}^c \sim G_A G_B$. The quantities $G_{A,B}$ are defined in Eq. (39) and their value given in Eq. (42). The quantities $L_{A,B}$ are defined by

$$L_{A,B} = \int \frac{d^2k}{(2\pi)^2} k^2 |F_{A,B}^0|^2. \tag{45}$$

The necessary integrations are performed with logarithmic accuracy. The L^3 behavior of the Born term is recovered. (Note that the full Racah result, see Eq. (16) in Sec. 3, contains terms proportional to L^2 and L also). The Coulomb corrections σ_A^c and σ_B^c agree with those of [36], see Eq. (29). They show the typical $L^2 = (\ln \gamma)^2$ behavior. A new result is the last term, σ_{AB}^c, where the Coulomb correction applies to both nuclei. It scales only with L. This shows, as discussed above, that it is smaller by a factor of L^2 compared to the Born result and therefore is less important in the high energy limit.

In a recent numerical calculation by Baltz et al. these results were checked by a calculation starting from the expression Eq. (30) directly and doing the integrations numerically [57,58,59,60,21]. We refer the reader to these papers for more details.

Calculations using the exact solution as given in [55,29] were already done for small impact parameter. As discussed above the size relation between the different terms is only true for the cross section, but not for the impact parameter dependent probability (see also Sec. 6 below). It was found that Coulomb corrections are present at small impact parameter. This can reduce the probability by up to 50%. These results were confirmed by a calculation in [61].

6 Higher Order Effects in Electron Pair Production: Multiple Pair Production and Bound-Free Pair Production

In the previous sections we have mainly dealt with one special kind of higher order effects, the so-called Coulomb corrections. By definition they describe the effect of higher order Coulomb interactions on the one-pair production. They are well understood in terms of the Bethe-Maximon theory, or, equivalently, the approach of summing Feynman diagrams [27]. Higher order interactions can also lead to a second kind of processes: multiple pair production. Multiple pair production is the most important process of this type and will be discussed in this section. There will also be Coulomb corrections to multiple pair production and we will see that they can be incorporated into the existing framework.

In the high energy limit discussed in Sec. 5 the oppositely charged electrons and positrons enter in a symmetric way. This is in contrast to the second order correction for large angle pair production of [43], see the discussion in Sec. 2. An obvious asymmetry also occurs when the positively charged nucleus interacts with the electron to form a bound state (K-,L-,... shell capture). This will be dealt with in Sec. 6.2. We conclude with some remarks regarding muon pair production. In this case the finite size of the nucleus needs to be taken into account, which then leads to differences in the importance of Coulomb corrections and multiple pair production cross sections as compared to the e^+e^- case.

6.1 Multiple pair production

In heavy ion collisions with $\eta \equiv \frac{Z_1 Z_2 e^2}{\hbar v} \gg 1$ a classical impact parameter b can be defined. At the high ion energies considered here the classical path can be taken as a straight line, see e.g. Chap. 2 of [17] or [23] for details. One can then calculate impact parameter dependent probabilities for pair production $P(b)$ in the semiclassical or Glauber approximations. The total cross section is given by the integration of this probability over all b.

There is a handy formula for the impact parameter dependent (single) pair production probability in $P^{(1)}$ in lowest order, as shown in [37]. Quasireal photons from each nucleus collide to produce an e^+e^--pair, the total cross section is denoted by $\sigma_{\gamma\gamma}(s)$, where s is the square of the c.m. energy. Using a simple version of the impact parameter dependent equivalent photon spectrum (valid for $1/m \ll b \ll \gamma/m$) and the relation $\int_{4m^2}^{\infty} \frac{ds}{s} \sigma_{\gamma\gamma}(s) = \frac{14\pi}{9} \frac{\alpha^2}{m^2}$ one obtains [53,62]

$$P^{(1)}(b) \approx \frac{28}{9\pi^2} \frac{Z_1^2 Z_2^2 \alpha^4}{m^2 b^2} \left[2\ln\gamma_{lab}^2 - 3\ln(mb) \right] \ln(mb) \quad \text{for } 1 \ll mb \ll \gamma_{lab}$$

$$\approx \frac{28}{9\pi^2} \frac{Z_1^2 Z_2^2 \alpha^4}{m^2 b^2} \left[\ln\frac{\gamma_{lab}^2}{mb} \right]^2 \quad \text{for } \gamma_{lab} \ll mb \ll \gamma_{lab}^2. \tag{46}$$

This equation displays nicely the dependence on the impact parameter b and the electron mass m. It also shows directly that for sufficiently large values of Z_1, Z_2 and γ_{lab} the first order probability $P^{(1)}(b)$ exceeds one, i.e., unitarity is violated. We further note that this calculation underestimates the probability in the range of small impact parameters $b \sim \lambdabar = \frac{\hbar}{mc}$. The equivalent photon approximation used to derive this approximation is not justified in this region. More exact numerical calculations need to be done.

The impact parameter dependent probability $P^{(1)}(b)$ in lowest order was calculated numerically in [63,64]. The quantity $P^{(1)}(b)$ found there is larger than the one given by Eq. (46), and values larger than one are possible at RHIC and LHC. As an example $P^{(1)}(b=0) = 3.9$ (1.6), and $P^{(1)}(\lambdabar) = 1.5$ (0.6) [63] for LHC (RHIC) are found.

The problem of the violation of the unitarity of $P(b)$, that is, that $P(b)$ will exceed unity for sufficiently large beam energies, was mentioned in [20]. It led to a series of studies starting around 1990. It was found that the production of multiple pairs in a single collision restores unitarity [65]. e^+e^--pair production at high energies can be studied in the sudden approximation, for not too large impact parameters and invariant masses. I.e., we can neglect the time-ordering operator in the Dyson-expansion of the S-matrix to get:

$$S = \exp(-i \int_{-\infty}^{\infty} V(t)dt). \tag{47}$$

One introduces the *pair* annihilation and creation operators b_i and $b_i^\dagger$, where i denotes collectively the state of the pair (momenta and spin projection). To a good approximation the pairs can be treated as "quasibosons" with the usual commutation relations:

$$[b_i, b_j^\dagger] = \delta_{ij}. \tag{48}$$

We can then write

$$\int_{-\infty}^{\infty} V(t)dt = \sum_i u_i b_i^\dagger + u_i^* b_i, \tag{49}$$

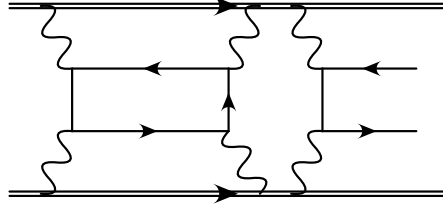where u_i is a c-number which describes the probability amplitude for the

Fig. 8. Third order contribution to the one-pair production.

production of a pair in state i in lowest order, see e.g. Sect. 7.1 of [20]. In principle, the interaction V also contains rescattering terms, i.e. terms, where the electron (or positron) of a pair changes its momentum and spin. We neglect these terms. We use the Baker-Campbell-Hausdorf identity

$$e^{A+B} = e^A e^B e^{-\frac{1}{2}[A,B]}, \tag{50}$$

which is valid for two operators A and B for which the commutator is a c-number. With this identity one can directly obtain an expression for the production of multiple pairs with given quantum numbers, valid to all orders. In Fig. 8 we show a third order contribution to the one-pair production. The other e^+e^- pair which is created is annihilated (by a "light-by-light scattering diagram"). This is quite similar to the emission of multiple soft photons due to a classical current, see e.g. [12]. One can say that a coherent state [66] of e^+e^- pairs is produced.

Similar approaches were followed in [67] and [68]. Another early work in this direction was given in [69,70]. All studies essentially make use of the "quasiboson" approximation, see Eq. (50) above. It is then found that the probability to produce N pairs $P(N,b)$ is given by a Poisson distribution:

$$P(N,b) = \frac{P^{(1)}(b)^N}{N!} \exp\left[-P^{(1)}(b)\right], \tag{51}$$

where $P^{(1)}(b)$, the probability for pair production calculated in lowest order (which can become larger than one). The quantity $P^{(1)}(b)$ acquires the meaning of the "average number of e^+e^- pairs" produced in a single ion collision:

$$\langle N(b) \rangle = \sum_N N P(N,b) = P^{(1)}(b). \tag{52}$$

Another approach without the use of the quasiboson approximation was done in [51] and later also in [71]. There it was found that quite generally the amplitude for N pair production by an external field is given by

$$S_N = \langle 0| S |0 \rangle \sum_\sigma \text{sgn}(\sigma) s^{+-}_{k_1 l_{\sigma(1)}} \cdots s^{+-}_{k_N l_{\sigma(N)}}, \tag{53}$$
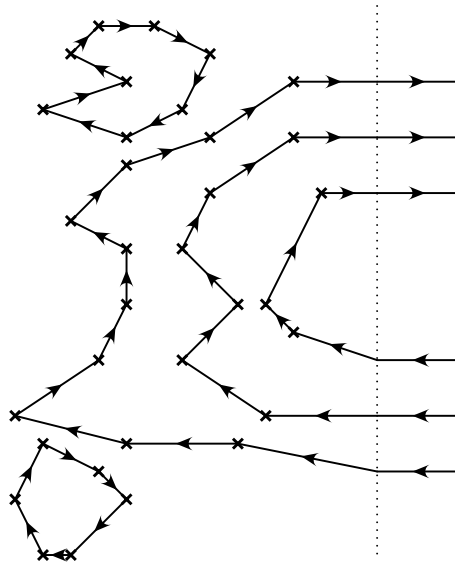
Fig. 9. Graphical illustration of the N-pair production process. The interaction with the external field is shown as crosses. The production of a pair is described by a fermion line coming from and leaving to the future, interacting an arbitrary number of times with the external field. The vacuum-vacuum amplitude $\langle 0| S |0\rangle$ corresponds to the sum of all closed fermion loops.

where k_i, l_i are the quantum numbers (momenta and spin projection) of electron and positron, respectively, and σ denotes a permutation of $\{1, \cdots, N\}$, see also Fig. 9. The vacuum-to-vacuum amplitude is present in all QED calculations, but is often dropped if it is of absolute value 1. Here this amplitude is < 1 and is due exactly to the contribution of all light-to-light diagrams, see Fig. 8. The amplitude s^{+-} is the one for the production of a single pair, corresponding to a single fermion line. Neglecting the antisymmetrisation of the amplitudes, one gets the N pair amplitude as the product of the vacuum-vacuum amplitude and the single-pair production amplitudes. From this one gets again a Poisson distribution for the N-pair production probability. As before the approximation introduced lead to an independence of each pair production process from all others, which is the essential ingredient needed to get the Poisson distribution. For further details we refer to Chap. 6 of [18].

With the impact parameter dependent probability $P^{(1)}(b)$ calculated, e.g., in [63,64] one can use Eq. (51) to obtain the probabilities for N-pair production $P(N, b)$, see Fig. 10. One can see that for impact parameters $b \approx 2R$ up to about $\lambdabar$ on the average 3–4 pairs will be produced in Pb-Pb collisions at the LHC. This means that each photon-photon event — especially those with high invariant mass, which occur predominantly at impact parameters close to $b \gtrsim 2R$ — is accompanied by the production of several (low-energy) e^+e^- pairs (most of them however will remain unobserved experimentally). Integrating over the impact parameter the total multiple pair production cross section was given in [72], see Fig. 11.
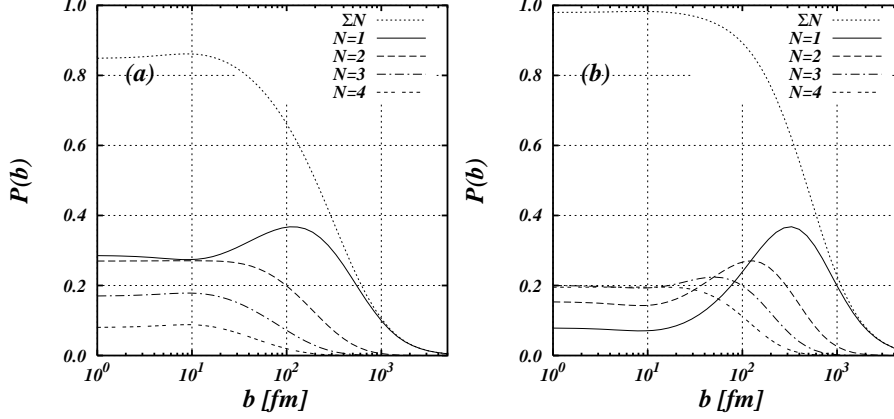
Fig. 10. The impact parameter dependent probability to produce N e^+e^--pairs ($N = 1, 2, 3, 4$) in one collision is shown for RHIC ($\gamma = 100$, Au-Au) (a) and for the LHC ($\gamma = 2950$, Pb-Pb) (b). Also shown is the total probability to produce at least one e^+e^--pair $\sum_{N=1}^{\infty} P(N, b) = 1 - P(0, b)$. One sees that at small impact parameters multiple pair production dominates over single pair production.
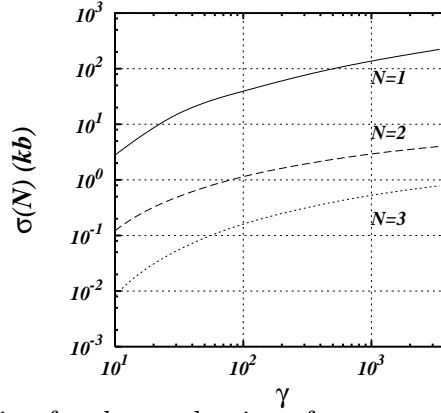

Fig. 11. Total cross section for the production of one, two and three pairs in PbPb collisions is shown as a function of the ion energy.

The Poisson distribution is also valid if, e.g., Coulomb corrections are included in the calculation of the single pair production. As seen in Eq. (53) they need to be taken into account for a single lepton line to get a $P^1(b)$ including Coulomb corrections. This $P^1(b)$ was calculated for the high energy limit, as discussed in Sec. 5, in [73,60,61]. It was found that the Coulomb correction reduce $P^1(b)$ up to 50%. The single pair production probability $P(b)$ falls off essentially as $1/b^2$. The total cross section is therefore dominated by large impact parameters and not very sensitive to the multiple pair production effects at small b. In [62] the reduction of the exclusive one-pair production cross section $\sigma(N = 1)$ was estimated to be -6.4% for RHIC and -4.7% for LHC, using the numerical results of [51,72].

Multiple pair production cross sections are dominated by impact parameters around $b \approx \lambdabar$. It would be of interest to establish this effect experimentally. In addition, Coulomb corrections are enhanced for these close collisions. At
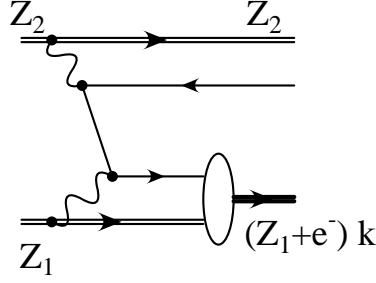
Fig. 12. Bound free pair production is the pair production process, where the electron is produced into a bound state of one of the ions.

the SPS (CERN) the effect was looked for, see [74], but only an upper bound could be given, which is still above the theoretical prediction. The possibilities at the LHC will be briefly discussed in 8.

6.2 Bound-free pair production

Bound-free pair production is the pair production process, where the electron is created in a bound state with one of the ions, say Z_1 (see Fig. 12)

$$Z_1 + Z_2 \rightarrow (Z_1 + e^-)_{K,L,...} + e^+ + Z_2. \tag{54}$$

Since our previous review [18] essentially no further calculations of bound-free pair production were made. The most careful state-of-the-art calculations were done in [42]. It is a Born-approximation calculation, using Dirac wave functions for the electrons and positrons in the field of a point nucleus with charge Z_1. In this approximation the cross-section scales with Z_2^2. At the high energies relevant for RHIC and LHC this is a good approximation, see also Sec. 8. Higher order processes of the class (iv) would lead to a deviation from the Z_2^2 scaling. They have been calculated using the ultrarelativistic limit of the Dirac equation in [75]. Only a small reduction of the order of 1% was found.

In an "Einstein special issue" electron-positron pair production in relativistic heavy ion-atom collisions was reviewed in [76] in a general way, not restricted to the high energy limit. In this paper a discussion of the bound-free pair production mechanisms is also given. While at the high energies the "excitation type" mechanism studied in [42] and in other papers dominates, the "transfer type" mechanism is also important at lower beam energies. "Excitation" here means, that the electron and the positron are best described by wave functions in the target Coulomb field, "transfer" means that the positron is in the Coulomb field of the target, whereas the electron is "transferred" to the Coulomb field of the projectile. For the lower beam energies it becomes

more proper to treat pair production by a two-center calculation. At high energies, 'class (iv)' is relatively unimportant, see above. On the other hand, at lower energies this type of process becomes increasingly important and causes further calculational complexities.

The cross-section for bound-free pair production at high energies rises only with $\ln \gamma$, i.e.,

$$\sigma = A \ln \gamma + B. \tag{55}$$

It is only a small fraction of the total cross section of free pair production, which rises with $(\ln \gamma)^3$. The parameters A and B have been given for various systems in [42]. Nevertheless, this process is an important one for the operation of the Pb-Pb beam at LHC: the ions which have captured an electron from the vacuum have a charge-to-mass-ratio different from the beam particles and they will hit the wall at a rather well defined 'hot spot'. This is discussed further in Sec. 8 below.

6.3 Higher order corrections to muon pair production

In this review we focus on the production of electron-positron pairs. Rather similar phenomena will appear in muon pair production, scaled with the corresponding mass. The larger muon mass has an effect on the different processes: in [27] it is remarked that the nucleus is an extended object with the inverse radius

$$\Lambda = \frac{1}{R} \sim 30 MeV. \tag{56}$$

At such scales the electric field differs substantially from the pure Coulomb behavior. This is especially of interest for muon pair production, where we have the inequality

$$m \ll \Lambda \ll m_\mu. \tag{57}$$

This means that a simple scaling of the cross section by m^2/m_μ^2 is not valid. It is shown in [27] that there is a suppression factor of Λ/m_μ for additional photon exchanges. This is because the form factor cuts out the short wavelength photons with $k > \Lambda$ and the remaining long-wavelength photons cannot resolve the dipole formed by the lepton pair which is of extension $\sim 1/m_\mu$. This leads to a reduction of the Coulomb effects for the muon case compared to the electron case. On the other hand unitarity corrections, due to the additional production of electron-positron pairs together with the muon-pair, is

enhanced. This can be understood as the impact parameter range in the muon pair case is much smaller than in the electron case and the probability to produce (additional) electron-positron pairs is then large. For further discussion we refer to [27].

7 Transition from the adiabatic to the sudden regime

The physics of e^+e^- pair production in fast ($v \approx c$) and slow ($v \approx 0$) heavy ion collisions ($Z_{\text{united atom}} > 137(173)$) is very different: for the slow collisions there is spontaneous pair production in supercritical fields, a non-perturbative effect. For fast collisions we can apply perturbation theory. Two-photon production dominates, as was discussed above. Let us first mention the corresponding situation of atomic ionization and electron-positron-pair production in a time-varying spatially-constant electric field of the form

$$\vec{E}(t) = \vec{E}_0 \cos \omega t. \tag{58}$$

The problem of ionization of atoms in a time varying electric field is very similar to the problem of e^+e^- pair production, which may be viewed as ionization of the negative energy Dirac sea, see Sec. 4. For ionization there is a similar transition from a slowly varying field to the high frequency case. The ionization of an H-atom in a time varying electric field is a textbook problem, see, e.g., p. 739ff, problem XVII in [77]. One limit — large frequency ω and a small field strength E_0 — is the usual photo-effect. The other limit is ionization in a static electric field. For a sufficiently strong static ($\omega = 0$) electric field, of the order of $E_a = \frac{m^2 e^5}{\hbar^4} \equiv E_c \alpha^3$, the electron disappears classically into the continuum; for lower field strength it can tunnel through the barrier, see, e.g., [78].

The critical atomic field strength E_a is given by the condition $eE_a a_B = \text{Ry}$, i.e., the work done in the field over the typical length scale (the Bohr radius a_B) is then equal to the typical energy scale (the ionization energy $\text{Ry} = e^2/(2a_B)$). (To obtain the critical field strength for the Schwinger case, discussed in Sec. 1, one needs to replace the Bohr radius by the Compton wavelength of the electron $\lambdabar = \hbar/(mc)$ and the Rydberg energy by the electron rest mass mc^2.) The field strength occurring in current lasers, see, e.g., [79] is strong enough to lead to such ionization processes: in Chap. VI of [79] the optical field ionization of atoms is reviewed. The important parameter which divides the strong field and the weak field limits is the Keldysh parameter γ_K (see Eq. (21) of [79]). For

$$1/\gamma_K \equiv \frac{eE_0 a_B}{\hbar \omega} \ll 1 \tag{59}$$

we have the perturbative limit, for

$$1/\gamma_K \gg 1 \tag{60}$$

we have the strong field regime. We do not go further into this but turn to e^+e^- pair production case, which was studied in [80].

The adiabaticity parameter (see also [13,14]) is given by Eq. (47) of [80]:

$$\gamma_{BI} = \frac{mc\omega}{eE}. \tag{61}$$

It corresponds to the Keldysh parameter γ_K of the atomic physics case. The Compton wave length of the electron λ, now replaces the Bohr radius a_B. Their final formula for the pair-production probability per unit time and volume is

$$w = \frac{\alpha E^2}{2\pi(g(\gamma_{BI}) + 1/2g'(\gamma_{BI}))} \exp(-\frac{\pi m^2}{eE} g(\gamma_{BI})). \tag{62}$$

The function $g(\gamma_{BI})$ is given by Eq. (45) of [15], it interpolates between the two extreme situations. In the limit $\gamma_{BI} \ll 1$ it is given by

$$g(\gamma_{BI}) = 1 - \frac{1}{8}\gamma_{BI}^2 + O(\gamma_{BI}^4) \tag{63}$$

and for $\gamma_{BI} \gg 1$ they find

$$g(\gamma_{BI}) = \frac{4}{\pi\gamma_{BI}} \ln(2\gamma_{BI}) + O(1/\gamma_{BI}). \tag{64}$$

The parameter γ_{BI} describes the transition from the high-field low-frequency limit ($\gamma_{BI} \ll 1$) to the low-field perturbative regime $\gamma_{BI} \gg 1$). In the $\gamma_{BI} \ll 1$ limit, one obtains the Schwinger formula, see Sec. 1. For $\gamma_{BI} \gg 1$ the perturbative result (see also Eq. (11) of [13,14]) is found:

$$\frac{d^4n}{d^3xdt} \sim \frac{c}{4\pi^3\lambda_e^4} \left(\frac{e^2 E}{4\hbar\omega}\right)^{\frac{4mc^2}{\hbar\omega}}. \tag{65}$$

It corresponds to n-th order perturbation theory, where n is the minimum number of quanta required to create an e^+e^- pair ($n \geq \frac{2mc^2}{\hbar\omega} \gg 1$).

For the heavy ion scattering the space-time dependence of the electric fields is much more complicated and one cannot obtain such instructive analytic results. Let us roughly estimate a parameter γ_{HI} for heavy ion collision corresponding to γ_{BI}: we put $\omega_{max} \sim 1/\Delta t = \frac{\gamma v}{b}$. With the maximum field strength $E \sim \frac{Ze\gamma}{b^2}$, see Eq. (3) in Sec. 1, we obtain:

$$\gamma_{HI} = \frac{mcbv}{Ze^2} = \frac{p_{el}}{\Delta p}, \tag{66}$$

38

where $p_{el} = mc$ is a typical electron momentum scale and $\Delta p = \frac{2Ze^2}{bv}$ corresponds to the momentum transfer in a Coulomb collision(see Eq. (4) in Sec. 1). For a typical impact parameter b one can take the Compton wave length of the electron, i.e., $b \approx \hbar/(mc)$. So we have

$$\gamma_{HI} = v/(Z\alpha). \tag{67}$$

In the relativistic case, $v \sim c$, this is ≥ 1, i.e., we are in the low-field high-frequency limit. For $v \ll 1$ we are in the strong-field non-perturbative limit.

Our conclusion from this chapter is the following: The slow collisions, with their static overcritical fields are in a different regime of the adiabaticity parameter as compared to the fast (ultra-) relativistic heavy ion collisions: the perturbative approach, (sometimes up to spectacularly high orders, see [23]) is well justified. The crossover between these two regimes can then be expected to occur in the region where the electron velocity is of the order of the velocity of the ions, i.e. $v \approx Z\alpha$, which corresponds to $\gamma \approx 1 \ldots 2$.

There is strong support for a future x-ray-free-electron laser at Desy (Hamburg), see [81] and one can expect exciting new results. The possibilities of optics in the relativistic regime, which are opened up by ultraintense laser pulses, are described in [82]. We mention the talk by A. Ringwald [83] or [13] and the theoretical calculations of pair creation in the fields of an X-ray free electron laser [84]. On the other hand, from what we said above, we have perturbative physics from the heavy ion collisions: the fields get very strong, with increasing ion energy, but, at the same time, the interaction time decreases in the same way.

8   Comparison to experiment and outlook to LHC

Since our last review of this subject in [18] the heavy ion collider RHIC has come into operation. Both the STAR and the PHENIX collaborations have published measurements on e^+e^- pair production. In the case of STAR the data was taken for events accompanied by nuclear breakup. In this way one is able to measure pair production at small impact parameters. Due to the high Lorentz factor γ, the electromagnetic fields are stronger than at SPS or AGS energies. For a discussion of experiments at these accelerators we refer to previous reviews [18,85,17]. As explained in Sec. 7 we are now in the perturbative limit. Also multiple pairs and bound free pair production processes can be measured in principle. It is the purpose of this section to give a short overview of these results and to compare them with the theoretical analysis, especially to the one done in [86]. Bound-free pair production was studied at RHIC as well. In the end we give a short outlook to the possibilities at the LHC.

8.1 e^+e^- pair production in ultraperipheral collisions at RHIC

The STAR collaboration has published data on e^+e^- pair production accompanied by nuclear breakup in ultraperipheral Au-Au collisions at a center of mass energy of 200 GeV per nucleon [38]. This process is illustrated in Fig. 13. The nuclear breakup of the gold ions is predominantly due to the electromagnetic excitation of the giant dipole resonance (GDR), see [18,17]. The breakup neutrons are detected in the ZDC (Zero Degree Calorimeter). It can be shown, that the amplitudes for these processes factorize [23] and that the cross section can be calculated by integrating the product of the probabilities over all impact parameters

$$\frac{d^6\sigma_{e^+e^-,GDR(n)}}{d^3p_+d^3p_-} = 2\pi \int\limits_{b_{min}}^{\infty} bdb(P_{GDR}(b))^n \frac{d^6P(b)}{d^3p_+d^3p_-},$$ (68)

where $P_{GDR}(b)$ denotes the probability of exciting one ion and $(P_{GDR}(b))^2$ is the probability to excite both ions. In this way pair production at small impact parameter can be selected. The average impact parameter is given approximately by [23]

$$\bar{b} = \frac{\int d^2b \, bP(b)}{\int d^2bP(b)} \approx \frac{8R_a}{3} \approx 19 \text{ fm},$$ (69)
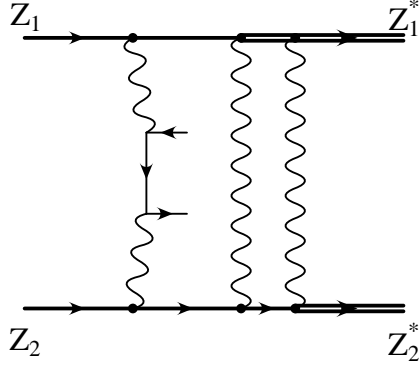
Fig. 13. At STAR pair production in connection with the electromagnetic excitation of one or both ions was measured.

The impact parameter dependent probability was calculated in lowest order in [86] based on the method developed in [63,87,72]. Only electrons and positrons with transverse momenta of $p_t > 60 MeV/c$ with rapidity $|y| < 1.15$ could be detected. This limited detector acceptance is taken into account in the calculation. Within the experimental accuracy a good agreement was found between the experimental and theoretical results not only for the total cross section but also for the distribution in energy and transverse momentum of electron and positron, see Figs. 14, 15 and 16 and in reference [38,88]. The results of the calculation agree also with a simpler calculation using the equivalent photon approximation in most cases. The exception is the distribution of the transverse momentum of the pair.

In the lowest order calculation electrons and positrons have an identical differential distribution. No asymmetry was also seen in the experimental data, which has a large statistical error. Also the total cross section was found to be in agreement with the lowest order calculation. No higher order reduction, as predicted by the Bethe-Maximon theory was observed, which should be a reduction of about 17%. But this is mainly due to the restriction on the phase space by the experiment, where these corrections are not expected.

8.2   Bound-free pair production at RHIC and the forthcoming LHC(Pb-Pb)

The bound-free pair production (BFPP) (see the discussion in Sec. 6.2) is a process which is of practical importance for the operation of the LHC in the Pb-Pb mode. An electron-positron pair is produced, where the electron is produced not as a free particle but into a bound atomic state of one of the ions,

$$Z_1 + Z_2 \rightarrow (Z_1 + e^-)_{1s_{1/2},\cdots} + e^+ + Z_2. \tag{70}$$
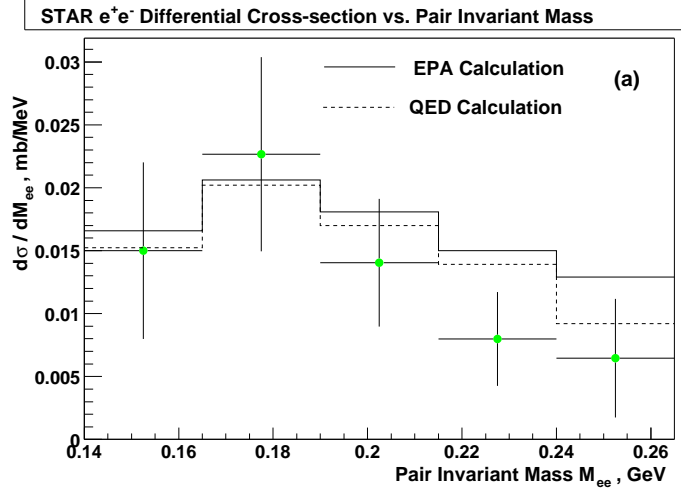
Fig. 14. Comparison of the distribution of the pair mass for the STAR experiment to the theoretical QED calculations of [86] and to a calculation using the equivalent photon approximation (EPA). Taken from [38]
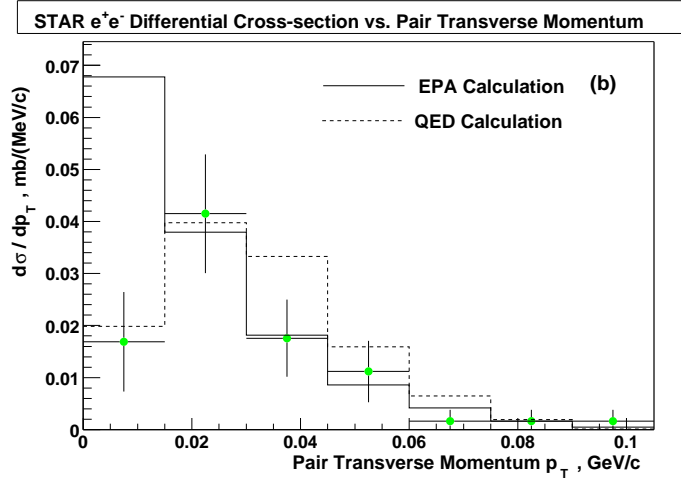

Fig. 15. Comparison of the transverse momentum distribution of the electron and the positron for the STAR experiment to the QED and the EPA calculation. Same as in Fig. 14. Taken from [38]

As this changes the charge state of the nucleus, it is lost from the beam in the collider. Together with the electromagnetic dissociation of the nuclei (see [18,17] these two processes are the dominant loss processes for heavy ion colliders. It has been realized [89], (see also [90,91]), that the BFPP process can also result in a localized beam-pipe heating: the atomic states are produced with a small perpendicular momentum of the order of m, and therefore leads to a narrow singly-charged ion beam (The process of electromagnetic dissociation is less severe in this respect as the momentum transfer to the ions is more spread out and the ions are not so strongly focussed on a single spot). These beams with altered magnetic rigidity will deposit their energy in a localized region of the beam pipe and cause a localized heating. This can lead to
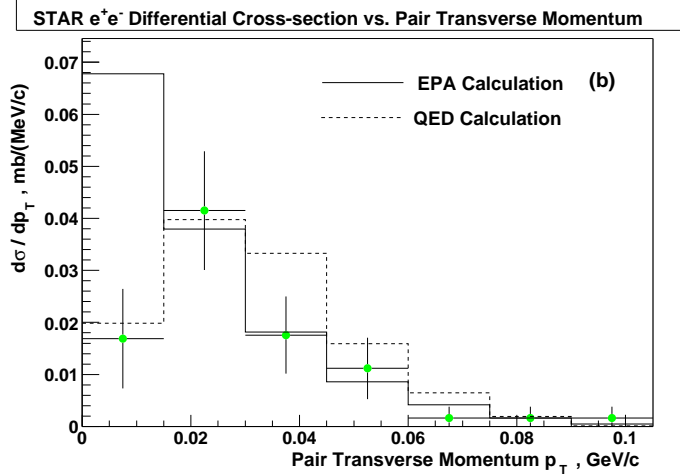
Fig. 16. Comparison of the transverse momentum distribution of the pair for the STAR experiment to the QED and the EPA calculation. Same as in Fig. 14. Taken from [38].

the quenching of the superconducting magnets. The energy deposited per unit time is of the order of Watts. This limits the luminosity of the Pb-Pb collider at LHC [90]. The effect of BFPP is studied more quantitatively through simulations of the ion showers in a dipole magnet in [92,93]. These calculations are based on the cross section given in [42]. In this reference, a comparison is also made with the results of other calculations. The authors of [92] conclude that "...the secondary beam of ions emerging from each collision point at the nominal peak luminosity $L = 1.0 \times 10^{27} cm^{-2}s^{-1}$ is not likely to quench a dipole magnet".

Due to the lower beam energy at RHIC, the energy deposit there is smaller and therefore not important as a limiting factor to the beam luminosity. However, it can serve as a testing ground for the theoretical numbers given in [42]. This is especially important, as the experimental result with the highest energies is from a fixed target measurement with an energy of 160 GeV per nucleon [94], corresponding to a $\gamma = 9.3$, still far away from the situation at the LHC.

First results of a measurement of ion beam losses due to BFPP in Cu-Cu collisions at RHIC were reported in [95]. Due to the small number of events observed the authors were not able to give a value for the cross section, but they conclude that within the uncertainties associated with the experimental conditions the data are consistent with the signal expected from BFPP. It is a valuable test of the ability to quantitatively predict the BFPP effect for the LHC.

8.3   Outlook on LHC

In [86] also an outlook to the situation for the LHC is given. One of the drawbacks of all possible measurements at high energies is the fact that pair production is predominantly produced in the forward direction, whereas the detectors are designed towards central events. But most of the interesting effects, like Coulomb correction and multiple pair production will occur at small transverse momenta. In [96] it is discussed how the very inner part of the detectors can be used for pair production detection. The limits of the transverse momentum can be reduced to $p_t > 2.6\text{MeV}$, which is comparable to the rest mass. This is explored in more detail in [86]. It is found that about 10% of all pairs produced together with nuclear excitation will come from multiple pair production.

Another approach has been studied in [97]. Here the very forward CASTOR detector is used to measure pair production. Calculations in lowest order are done and it is proposed to use this as a luminosity measurement for the LHC. Of course the accuracy of such a luminosity measurement relies on the precise theoretical knowledge of this process especially in this region and how large Coulomb correction contribute to it. In combination with the nuclear excitation of the ions it would also allow to study pair production at small impact parameters.

9 Conclusion

In April 1990 a workshop took place in Brookhaven with the title 'Can RHIC be used to test QED?' [98]. We think that after about 17 years the answer to this question is 'no'. However, many theorists were motivated to deal with this topic. The gradual progress which was sometimes quite tortuous, is described in this report.

In this review we studied electron-positron pair production in heavy ion collisions at relativistic energies. There were quite a few papers in the last years approaching this topic from various aspects. Whereas the lowest order Born result was known for a long time, higher order (Coulomb) corrections have been under debate for the last decades. These corrections were studied using various methods. One of these methods follow the approach of Bethe and Maximon, which was used to study Coulomb corrections to the pair production in photon-nucleus interactions (the Bethe-Heitler process). QED perturbation theory was also used and it was shown [27] that they yield the same result as the approach of Bethe and Maximon. Difficulties with obtaining analytical solutions appear when more than one photon are attached to each nucleus, and no firm results have been obtained up to now. However, for the total cross section these effects are small.

It has been found in theoretical calculations that higher order effects can be quite sizeable for collisions where small impact parameters are selected. But an experimental confirmation has not been made up to now.

The fields occurring in ultrarelativistic heavy ion collisions are very strong. So one may expect that some new kind of nonperturbative effects could arise, similar to the Schwinger mechanism for static electric fields. But the fields in the relativistic heavy ion collision act only for a short time and higher order perturbation theory is appropriate. We also discuss the problem of the transition from slow to fast collisions. However, this chapter is far from being solved. A new higher order effect in relativistic heavy ion reactions is the emission of multiple pairs in a single collision. This is quite a spectacular effect and it would be of some interest to observe it experimentally in forthcoming experiments at the LHC.

In addition to the intrinsic interest of the theoretical study of pair production at high energies there is the practical importance of these processes in the more general study of ultraperipheral processes. Pair production is a background process, e.g., to vector meson photoproduction. The very large cross section for bound-free pair production limits the maximum Pb-Pb luminosity at the forthcoming LHC. Thus it is mandatory to understand these QED effects to a high degree of accuracy.

Finally, we review the experimental results on pair production at RHIC and their theoretical interpretation. Results on the bound-free pair production mechanism obtained recently at RHIC are also discussed. Agreement with theory is good, and we expect a similar good agreement at the forthcoming LHC. This good agreement is of course also the reason why electron and muon pairs produced in ultraperipheral collisions may well be used to monitor the luminosity at colliders. This should not be surprising since QED is the best-tested theory we have.

Acknowledgements

References

[1] J. S. Schwinger, Phys. Rev. **76**, 790 (1949).

[2] R. P. Feynman, Phys. Rev. **76**, 749 (1949).

[3] R. P. Feynman, Phys. Rev. **76**, 769 (1949).

[4] J. S. Schwinger (Editor), *Selected Papers on QED* (Dover, New York, 1958).

[5] C. D. Anderson, Phys. Rev. **43**, 491 (1933).

[6] L. D. Landau and E. M. Lifshitz, Phys. Z. Sowjet. **6**, 244 (1934).

[7] G. Racah, Nuovo Cim. **14**, 93 (1937).

[8] V. M. Budnev, I. F. Ginzburg, G. V. Meledin, and V. G. Serbo, Phys. Rept. **15**, 181 (1974).

[9] J. Rafelski, L. P. Fulcher, and A. Klein, Phys. Reports **38C**, 227 (1978).

[10] W. Greiner, B. Müller, and J. Rafelski, *Quantum Electrodynamics of Strong Fields* (Springer Verlag, Berlin, 1985).

[11] J. S. Schwinger, Phys. Rev. **82**, 664 (1951).

[12] C. Itzykson and J.-B. Zuber, *Quantum Field Theory* (McGraw-Hill, Singapore, 1980).

[13] A. Ringwald, in *Electromagnetic probes of fundamental physics*, edited by W. Marciano and S. White (World Scientific Publishing Company, Singapore, 2003), p. 67.

[14] A. Ringwald, Phys. Lett. **B510**, 107 (2001).

[15] E. Brezin and C. Itzykson, Phys. Rev. **D2**, 1191 (1970).

[16] F. Krauss, M. Greiner, and G. Soff, Prog. Part. Nucl. Phys. **39**, 503 (1997).

[17] G. Baur, K. Hencken, and D. Trautmann, J. Phys. **G24**, 1657 (1998).

[18] G. Baur *et al.*, Phys. Rept. **364**, 359 (2002).

[19] C. A. Bertulani, S. R. Klein, and J. Nystrand, Ann. Rev. Nucl. Part. Sci. **55**, 271 (2005).

[20] C. A. Bertulani and G. Baur, Phys. Rept. **163**, 299 (1988).

[21] A. Baltz *et al.*, Photoproduction at collider energies: From RHIC and HERA to the LHC, hep-ph/0702212, 2007.

[22] Workshop on Photoproduction at collider energies: from RHIC and HERA to LHC, http://dde.web.cern.ch/dde/photoprod_ect07/.

[23] G. Baur *et al.*, Nucl. Phys. **A729**, 787 (2003).

[24] H. A. Bethe and L. C. Maximon, Phys. Rev. **93**, 768 (1954).

[25] H. Davies, H. A. Bethe, and L. C. Maximon, Phys. Rev. **93**, 788 (1954).

[26] L. D. Landau and E. M. Lifschitz, *Quantenelektrodynamik*, No. IV in *Lehrbuch der theoretischen Physik* (Akademie Verlag, Berlin, 1986).

[27] D. Ivanov and K. Melnikov, Phys. Rev. **D57**, 4025 (1998).

[28] H. Meier, K. Hencken, D. Trautmann, and G. Baur, Eur. Phys. J. **C2**, 741 (1998).

[29] A. J. Baltz and L. D. McLerran, Phys. Rev. **C58**, 1679 (1998).

[30] A. J. Baltz, F. Gelis, L. D. McLerran, and A. Peshier, Nucl. Phys. **A695**, 395 (2001).

[31] B. Segev and J. C. Wells, Phys. Rev. **A57**, 1849 (1998).

[32] B. Segev and J. C. Wells, Phys. Rev. **C59**, 2753 (1999).

[33] A. Aste *et al.*, Eur. Phys. J. **C23**, 545 (2002).

[34] A. J. Baltz, Phys. Rev. **C71**, 024901 (2005).

[35] U. Eichmann, J. Reinhardt, S. Schramm, and W. Greiner, Phys. Rev. **A59**, 1223 (1999).

[36] D. Y. Ivanov, A. Schiller, and V. G. Serbo, Phys. Lett. **B454**, 155 (1999).

[37] R. N. Lee, A. I. Milstein, and V. G. Serbo, Phys. Rev. **A65**, 022101 (2002).

[38] J. Adams *et al.*, Phys. Rev. **C70**, 031902 (R) (2004).

[39] http://www.euler-2007.ch.

[40] R. N. Lee, A. I. Milstein, and V. M. Strakhovenko, Phys. Rev. **A69**, 022708 (2004).

[41] A. W. Aste, K. Hencken, D. Trautmann, and G. Baur, Phys. Rev. **A50**, 3980 (1994).

[42] H. Meier *et al.*, Phys. Rev. **A63**, 032713 (2001).

[43] S. J. Brodsky and J. Gillespie, Phys. Rev. **173**, 1011 (1968).

[44] E. Bartos, S. R. Gevorkyan, E. A. Kuraev, and N. N. Nikolaev, Phys. Rev. **A66**, 042720 (2002).

[45] E. Bartos, S. R. Gevorkyan, E. A. Kuraev, and N. N. Nikolaev, J. Exp. Theor. Phys. **100**, 645 (2005).

[46] S. R. Gevorkyan and E. A. Kuraev, J. Phys. **G29**, 1227 (2003).

[47] E. Bartos, S. R. Gevorkyan, E. A. Kuraev, and N. N. Nikolaev, Phys. Lett. **B538**, 45 (2002).

[48] S. R. Gevorkyan and A. V. Tarasov, Challenge of lepton pair production in peripheral collisions of relativistic ions, hep-ph/0512098, 2005.

[49] A. J. Baltz, M. J. Rhoades-Brown, and J. Weneser, Phys. Rev. A **44**, 5569 (1991).

[50] *Coulomb Excitation, Perspectives in Physics*, edited by K. Alder and A. Winther (Academic Press, New York, London, 1966).

[51] K. Hencken, D. Trautmann, and G. Baur, Phys. Rev. **A51**, 998 (1995).

[52] I. Biallynicki-Birula and Z. Bialynicki-Birula, *Quantum Electrodynamics* (Pergamon 1975).

[53] R. N. Lee and A. I. Milstein, Phys. Rev. **A61**, 032103 (2000).

[54] R. N. Lee and A. I. Milstein, Phys. Rev. **A64**, 032106 (2001).

[55] B. Segev and J. C. Wells, Phys. Rev. **C59**, 2753 (1999).

[56] M. Abramowitz and I. A. Stegun, *Handbook of mathematical Functions* (Dover, New York, 1965).

[57] A. J. Baltz, Phys. Rev. **C71**, 024901 (2005).

[58] A. J. Baltz, Phys. Rev. **C68**, 034906 (2003).

[59] A. J. Baltz, Acta Phys. Hung. **A27**, 323 (2006).

[60] A. J. Baltz, Phys. Rev. **C74**, 054903 (2006).

[61] R. N. Lee and A. I. Milstein, J. Exp. Theor. Phys. **104**, 423 (2007).

[62] R. N. Lee, A. I. Milstein, and V. G. Serbo, Structure of the Coulomb and unitarity corrections to the cross-section of e+ e- pair production in ultrarelativistic nuclear collisions, 2001.

[63] K. Hencken, D. Trautmann, and G. Baur, Phys. Rev. **A51**, 1874 (1995).

[64] M. C. Güçlü *et al.*, Phys. Rev. A **51**, 1836 (1995).

[65] G. Baur, Phys. Rev. **A42**, 5736 (1990).

[66] R. J. Glauber, Phys. Rev. **131**, 2766 (1963).

[67] M. J. Rhoades-Brown and J. Weneser, Phys. Rev. A **44**, 330 (1991).

[68] C. Best, W. Greiner, and G. Soff, Phys. Rev. A **46**, 261 (1992).

[69] A. D. Erlykin, in *14th Int. Cosmic Ray Conf., München, Conf. Papers*, Vol. 6, p. 1987.

[70] A. D. Erlykin, in *14th Int. Cosmic Ray Conf., München, Conf. Papers*, Vol. 7, p. 2173.

[71] A. J. Baltz, F. Gelis, L. D. McLerran, and A. Peshier, Nucl. Phys. **A695**, 395 (2001).

[72] A. Alscher, K. Hencken, D. Trautmann, and G. Baur, Phys. Rev. **A55**, 396 (1997).

[73] K. Hencken, D. Trautmann, and G. Baur, Phys. Rev. **C59**, 841 (1999).

[74] C. R. Vane *et al.*, Phys. Rev. A **56**, 3682 (1997).

[75] A. J. Baltz, Phys. Rev. Lett. **78**, 1231 (1997).

[76] J. Eichler, Phys. Lett. **A347**, 67 (2005).

[77] A. Messiah, *Quantum Mechanics, Vol. II* (Nort-Holland Publishing Company, 1964).

[78] H. A. Bethe and E. E. Salpeter, *Quantum Mechanics of One- and Two-Electron Atoms* (Plenum, New York, 1977).

[79] T. Brabec and F. Krausz, Rev. Mod. Phys. **72**, 545 (2000).

[80] E. Brezin and C. Itzykson, Phys. Rev. D **2**, 1191 (1970).

[81] A. Merkel, Science **313**, 147 (2006).

[82] G. A. Mourou, T. Tajima, and S. V. Bulanov, Reviews of Modern Physics **78**, 309 (2006).

[83] Jena, Mai 2004 Kolloqium, http://desy.de/ ringwald/xfel/talks.

[84] R. Alkofer *et al.*, Phys. Rev. Lett. **87**, 193902 (2001).

[85] J. Eichler, Physics Report **193**, 165 (1990).

[86] K. Hencken, G. Baur, and D. Trautmann, Phys. Rev. **C69**, 054902 (2004).

[87] K. Hencken, D. Trautmann, and G. Baur, Phys. Rev. **A49**, 1584 (1994).

[88] V. B. Morozov, Electron positron production in ultra-peripheral heavy-ion collisions with the STAR experiment, nucl-ex/0403002, 2003.

[89] S. R. Klein, Nucl. Instrum. Meth. **A459**, 51 (2001).

[90] D. Brandt, Review of the LHC Ion Report, LHC Project Report 450, 2000.

[91] J. B. Jeanneret, Electron capture in Pb-Pb collisions and quench limit, Beam Physics Note 41, 2000.

[92] R. Bruce, S. Gilardone, and J. M. Jowett, bound free pair production loss and quench limit for LHC magnets, LHC Note 379, 2006.

[93] J. M. Jowett, R. Bruce, and S. S. Gilardoni, Luminosity limit from bound-free pair production in the LHC, Prepared for Particle Accelerator Conference (PAC 05), Knoxville, Tennessee, 16-20 May 2005.

[94] H. F. Krause *et al.*, Phys. Rev. Lett. **80**, 1190 (1998).

[95] J. M. Jowett *et al.*, Measurement of ion beam losses due to bound-free pair production in RHIC, Prepared for European Particle Accelerator Conference (EPAC 06), Edinburgh, Scotland, 26-30 Jun 2006, see http://accelconf.web.cern.ch/AccelConf/e06/PAPERS/MOPLS010.PDF.

[96] K. Hencken, Y. Kharlov, and S. Sadovsky, Ultraperipheral Trigger in ALICE, ALICE Internal Note ALICE-INT-2002-11, 2002.

[97] D. Bocian and K. Piotrzkowski, Acta Phys. Polon. **B35**, 2417 (2004).

[98] M. Fatyga, M. Rhoades-Brown, and M. Tannenbaum, Can RHIC be used to test QED: Workshop summary, Workshop "Can RHIC be used to test QED?", Upton, N.Y., Apr 20-21, 1990, BNL 52247 Formal Report.